PROGRESS REPORT

The Estimation of Atmospheric Dispersion at Nuclear Reactor Plants Utilizing Real Time Anemometer Statistics

by

Wen-Whai Li* and Robert N. Meroney**

prepared for

Site Safety Research Branch
Office of Nuclear Regulatory Research
U.S. Nuclear Regulatory Commission
Washington, D.C. 20555

*Graduate Research Assistant, Department of Civil Engineering
**Professor, Department of Civil Engineering

July 1982 CER82-83WWL-RNM1

TABLE OF CONTENTS

Chapter		Page
	LIST OF TABLES	iii
	LIST OF FIGURES	v
	LIST OF SYMBOLS	vi
1	INTRODUCTION	1
	1.1 STATEMENT OF WORK	1
	1.2 INTRODUCTION TO THE REPORT	2
2	LITERATURE REVIEW	3
	2.0 INTRODUCTION	3
	2.1 STATISTICAL THEORY BY CONTINUOUS MOVEMENTS	3
	2.2 RELATION BETWEEN LAGRANGIAN AUTOCORRELATION AND EULERIAN CORRELATION	7
	2.2.1 Linear-Correlation Method	7
	2.2.2 Moving-Frame Autocorrelation Method	8
	2.2.3 Probability Method	9
	2.2.4 Averaging Method	10
	2.3 STOCHASTIC PROCESS OF PARTICLE MOTION	11
3	APPROACH AND PROCEDURE	14
	3.0 INTRODUCTION	14
	3.1 EESTIMATION OF LAGRANGIAN AAUTOCORRELATION FUNCTION	14
	3.2 DIFFUSION EQUATION	16
	3.3 THE APPROACH	20
4	PRESENT DEVELOPMENT	21
	4.0 INTRODUCTION	21
	4.1 WIND TUNNEL	21
	4.2 CORRELATION MEASUREMENTS	22
	4.3 DIFFUSION MEASUREMENTS	24
5	SUMMARY AND FURTHER DEVELOPMENT	27
	5.1 SUMMARY	27
	5.2 FURTHER DEVELOPMENT	29
	REFERENCES	31
	TABLES	35
	FIGURES	55

LIST OF TABLES

Table		Page
1	A computational numerical scheme of calculating the Lagrangian autocorrelation function (Program EULLAG) . .	36
2	Summary of previous diffusion measurements conducted in the Meteorological Wind Tunnel	39
3	Characteristics of the simulated atmospheric boundary layer	40
4	Aparatus set up for velocity correlation measurements .	41
5	Comparison of the Lagrangian time scale	42
6	Dispersion data in the anisotropic homogeneous shear flow, $x_{1s} = 0$, $x_{2s} = 0$, $x_{3s} = 10$ cm, $x_1 = 100$ cm, $U_\infty = 200$ cm/sec	43
7	Dispersion data in the anisotropic homogeneous shear flow, $x_{1s} = 0$, $x_{2s} = 0$, $x_{3s} = 10$ cm, $x_1 = 200$ cm, $U_\infty = 200$ cm/sec	44
8	Dispersion data in the anisotropic homogeneous shear flow, $x_{1s} = 0$, $x_{2s} = 0$, $x_{3s} = 10$ cm, $x_1 = 500$ cm, $U_\infty = 200$ cm/sec	45
9	Dispersion data in the isotropic homogeneous shear flow, $x_{1s} = 0$, $x_{2s} = 0$, $x_{3s} = 10$ cm, $x_1 = 100$ cm, $U_\infty = 200$ cm/sec	46
10	Dispersion data in the isotropic homogeneous shear flow, $x_{1s} = 0$, $x_{2s} = 0$, $x_{3s} = 10$ cm, $x_1 = 200$ cm, $U_\infty = 200$ cm/sec	47
11	Dispersion data in the isotropic homogeneous shear flow, $x_{1s} = 0$, $x_{2s} = 0$, $x_{3s} = 10$ cm, $x_1 = 500$ cm, $U_\infty = 200$ cm/sec	48
12	Dispersion data in the anisotropic homogeneous shear flow, $x_{1s} = 0$, $x_{2s} = 0$, $x_{3s} = 20$ cm, $x_1 = 100$ cm, $U_\infty = 200$ cm/sec	49
13	Dispersion data in the anisotropic homogeneous shear flow, $x_{1s} = 0$, $x_{2s} = 0$, $x_{3s} = 20$ cm, $x_1 = 200$ cm, $U_\infty = 200$ cm/sec	50

Table		Page
14	Dispersion data in the anisotropic homogeneous shear flow, $x_{1s} = 0$, $x_{2s} = 0$, $x_{3s} = 20$ cm, $x_1 = 500$ cm, $U_\infty = 200$ cm/sec	51
15	Dispersion data in the isotropic homogeneous shear flow, $x_{1s} = 0$, $x_{2s} = 0$, $x_{3s} = 20$ cm, $x_1 = 100$ cm, $U_\infty = 200$ cm/sec	52
16	Dispersion data in the isotropic homogeneous shear flow, $x_{1s} = 0$, $x_{2s} = 0$, $x_{3s} = 20$ cm, $x_1 = 200$ cm, $U_\infty = 200$ cm/sec	53
17	Dispersion data in the isotropic homogeneous shear flow, $x_{1s} = 0$, $x_{2s} = 0$, $x_3 s = 20$ cm, $x_1 = 500$ cm, $U_\infty = 200$ cm/sec	54

LIST OF FIGURES

Figure		Page
1	Mean velocity profiles and turbulent intensity profiles, U_∞ = 200 cm/sec	56
2	Mean velocity profiles and turbulent intensity profiles, U_∞ = 300 cm/sec	57
3	Mean velocity profiles and turbulent intensity profiles, U_∞ = 500 cm/sec	58
4	Lateral distribution of mean velocity profiles at 80 cm height	59
5	Longitudinal space correlation at 10 cm height, U_∞ = 200 cm/sec	60
6	Transverse space correlation at 10 cm height, U_∞ = 200 cm/sec	61
7	Vertical space correlation at 10 cm height, U_∞ = 200 cm/sec	62
8	Longitudinal space correlation at 20 cm height, U_∞ = 200 cm/sec	63
9	Transverse space correlation at 20 cm height, U_∞ = 200 cm/sec	64
10	Vertical space correlation at 10 cm height, U_∞ = 200 cm/sec	65
11	Longitudinal autocorrelation at 10 cm and 20 cm height	66
12	Longitudinal space-time correlation with transverse separations	67
13	Longitudinal space-time correlation at 10 cm height, U_∞ = 200 cm/sec	68
14	Longitudinal space-time correlation at 20 cm height, U_∞ = 200 cm/sec	69
15	Normalized longitudinal space-time correlation versus τ/T_s	70
16	Properties of Eulerian models employed in the independent hypothesis analysis	71
17	Lagrangian scale as a function of the Eulerian parameter	72

LIST OF SYMBOLS

Symbol	Definition	Units
$\bar{c}$	mean concentration	$ppm \cdot L^{-3}$
dx_i	spatial increment	L
f(r)	spatial longitudinal velocity correlation	——
gamma	gamma function	——
g(r)	spatial lateral velocity correlation	——
i	turbulent intensity	——
K_{ij}	eddy diffusivity tensor	L^2T^{-1}
L	Lagrangian length scale	L
N(a,b)	Normal distribution with mean a and variance b	——
n	exponent in power law velocity profile	——
n(t)	random signal with o mean and variance $[u^2]$	——
Q	source flow rate	$ppm\ T^{-1}$
E^{R}_{ij}	Eulerian autocorrelation tensor	——
L^{R}_{ij}	Lagrangian correlation tensor	——
r	spherical coordinate	L
$_iT_E$	Eulerian time scale in the x_i direction	T
$_iT_L$	Lagrangian time scale in the x_i direction	T
T_s	Eulerian space-time scale	T
t	dispersion time	T
t*	non-dimensional time variable, τ/T_s	——
U	velocity	LT^{-1}
$\bar{U}$	local mean velocity	LT^{-1}
U_∞	free-stream velocity	LT^{-1}
u	longitudinal turbulent velocity	LT^{-1}
u_{ii}	turbulent velocity tensor	LT^{-1}

Symbol	Definition	Units
$W(x_i,\tau)$	probability density function of find a fluid particle in space x_i and $x_i + dx_i$ at any time	——
X_i^2	mean square particle displacement in x_i-direction	L^2
x_i	spacial coordinates	L
x_{is}	coordinates of point source	L
Δx_i	spatial separation in the x_i direction	L
Z_o	effective roughness height	L

Greek Symbols

α	Eulerian parameter, $\alpha = \sqrt{\overline{u'^2}}\ T_s/L$	——
β	ratio of the Lagrangian to the Eulerian time scale $\beta = {}_L T_1 / {}_E T_1$	——
β'	inverse of ${}_1 T_L$	T^{-1}
Γ	velocity gradient	T^{-1}
δ	boundary layer thickness	L
ξ	non-dimensional space variable, r/L	——
σ_s	plume standard deviation	L
τ	time increment	T
overbar	Eulerian time average	
sub ij	turbulence component	
[ ]	ensemble average	

1. INTRODUCTION

1.1 STATEMENT OF WORK

The dispersive nature of turbulent flow is an object of consideration in many branches of engineering and applied science. Reliable predictive relations applicable to a broad range of scales are not yet known. Indeed, most atmospheric transport predictive schemes for a nuclear reactor site still depend upon relating mean wind field characteristics measured at a particular site to regression formulae developed from data collected at other sites at other times.

Recent research on the turbulent dispersion phenomenon suggest that the concentration field in a wide variety of situations can be generated if the Lagrangian statistics properties are known. Unfortunately, due to the difficulty involved in initially tagging the particles in a manner which does not influence their future behavior, the tremendous work involved in obtaining necessary trajectories, and the subsequent laborious data analyses, it is not possible to obtain the Lagrangian statistics by tracking individual particles. Attempts have been made to deduce the Lagrangian autocorrelation from the Eulerian turbulent velocity at fixed points in space. Most of the attempts were based on the assumption that the Lagrangian autocorrelation and the Eulerian correlation, or Eulerian space-time cross correlation, are of similar shape but different scales. It is the purpose of this research to demonstrate how a systematic scheme based on a probability method can estimate these Lagrangian statistical measurements by a few anemometers located in the fixed Eulerian frame of reference.

Of course the major intent of this research is to predict the dispersive phenomenon in the atmospheric boundary layer. A meteorological wind tunnel was used to simulate an atmospheric boundary layer to provide velocity correlation measurements and diffusion measurements. An inhomogeneous turbulence field complicates the mathematical description of the turbulent mechanism; hence, most statistical theories assume a homogeneous wind field. As a first estimate of the atmospheric dispersion, we use a homogeneous statistical turbulent diffusion theory even though inhomogenuity and nonisotropy exist.

1.2 INTRODUCTION TO THE REPORT

The statistical theory by continuous movements and the relation between Lagrangian autocorrelation and Eulerian autocorrelation are reviewed in Chapter 2. Chapter 3 presents the estimation of Lagrangian statistics from the measured Eulerian statistics. The Baldwin and Johnson approach to the Lagrangian statistics is also displayed. The related dispersion solution in a sheared flow are presented. Present developments in the wind tunnel of the velocity correlation measurements and the diffusion measurements are shown in Chapter 4. A brief summary and suggestions for further development are included in Chapter 5.

Only one set of data for a fixed mean wind were analyzed for this report. Further data analysis will be completed in the near future.

2. LITERATURE REVIEW

2.0 INTRODUCTION

The basic theoretical approaches to statistical turbulent diffusion theory are either Lagrangian or Eulerian. The Lagrangian approach follows the statistical motion of a single particle, while the Eulerian approach concentrates on the balance of particle fluxes through a fixed point in the fluid and is normally simplified by the gradient-transfer theory (or K theory).

The statistical theory by continuous movements is described in Section 2.1. Section 2.2 presents several models proposed by different authors to obtain the Lagrangian statistics from the Eulerian statistics. A recently developed stochastic process model to deal with the turbulent diffusion problem is discussed in Section 2.3.

2.1 STATISTICAL THEORY BY CONTINUOUS MOVEMENTS

Diffusion of a fluid particle in a stationary, homogeneous turbulent flow without mean gradients was described in terms of Lagrangian velocities by Taylor (1921). The mean square particle displacement depends on the Lagrangian velocity variance and the Lagrangian autocorrelation

$$[X_i^2(t)] = 2[u_{ii}^2] \int_o^t \int_o^{t'} {}_L R_{ii}(\tau)\, d\tau\, dt' \quad , \tag{1}$$

where the square bracket indicates an ensemble average of N fluid particles and ${}_L R_{ii}(\tau)$ is a normalized Lagrangian autocorrelation function

$${}_L R_{ii}(\tau) = \frac{[u_{ii}(t)\, u_{ii}(t+\tau)]}{[u_{ii}^2]} \quad . \tag{2}$$

When Eq. (1) is integrated by parts, the Taylor's relation can be expressed in the Kampe de Feriet form, i.e.,

$$[X_i^2(t)] = 2[u_{ii}^2] \int_o^t (t - \tau)\, {}_LR_{ii}(\tau)d\tau \quad . \tag{3}$$

Based on Eq. (3), two obvious results can be seen:

(i) Within a very short dispersive range, ${}_LR_{ii}(\tau)$ approaches unity for a very short time lag so that

$$[X_i^2(t)] \cong [u_{ii}^2]t^2 \quad .$$

(ii) For a long range dispersion, ${}_LR_{ii}(\tau)$ approaches a constant value ${}_iT_L$,

$${}_iT_L = \int_o^\infty {}_LR_{ii}(\tau)d\tau \quad , \tag{4}$$

and since ${}_LR_{ii}(\tau)$ approaches zero for a very large time lag,

$$[X_i^2(t)] \cong 2[u_{ii}^2]\ {}_iT_L\ t \quad , \tag{5}$$

where ${}_iT_L$ is referred to as Lagrangian integral time scale and is an indication of the size of the largest eddy within the turbulent flow.

In a turbulent flow with uniform shear Γ and mean velocity $\bar{U}$, $\bar{U} = \Gamma x_3$, Corrsin (1953) derived expressions of the following form for the components of the dispersion tensor $[X_i(t)\ X_j(t)]$:

$$[X_1^2(t)] = \Gamma^2 \underbrace{[u_{33}^2] \{\frac{2}{3} t^3 \int_o^t {}_L R_{33}(\tau)d\tau - t^2 \int \tau {}_L R_{33}(\tau)d\tau}_{I}$$

$$\underbrace{+ \frac{1}{3} \int \tau^3 {}_L R_{33}(\tau)d\tau\}}_{} + 2 \underbrace{[u_{11}^2] \int_o^t (t - \tau) {}_L R_{11}(\tau)dt}_{II}$$

$$\underbrace{+ \Gamma^2 [u_{11}^2]^{\frac{1}{2}} [u_{33}^2]^{\frac{1}{2}} \int_o^t (t - \tau)^2 {}_L R_{31}(\tau)d\tau}_{III}$$

$$\underbrace{+ \Gamma^2 [u_{11}^2]^{\frac{1}{2}} [u_{33}^2]^{\frac{1}{2}} \int_o^t (t^2 - \tau^2) {}_L R_{13}(\tau)d\tau}_{} \quad , \tag{6}$$

$$[X_1(t)\ X_3(t)] = \Gamma \underbrace{[u_{33}^2] \int_o^t t(t - \tau) {}_L R_{33}(\tau)d\tau}_{I} +$$

$$\underbrace{[u_{11}^2]^{\frac{1}{2}} [u_{33}^2]^{\frac{1}{2}} \int_o^t (t - \tau) \{{}_L R_{13}(\tau) + {}_L R_{31}(\tau)\}d\tau}_{II}, \tag{7}$$

$$[X_2^2(t)] = 2[u_{22}^2] \int_o^t (t - \tau) {}_L R_{22}(\tau)d\tau \quad , \text{ and} \tag{8}$$

$$[X_3^2(t)] = 2[u_{33}^2] \int_o^t (t - \tau) {}_L R_{33}(\tau)d\tau \quad . \tag{9}$$

Notice that the shear enhanced term (I) in Eq. (6) and Eq. (7) dominate the long time dispersion ($t > {}_i T_L$). The turbulent shear correlation contribution term, (III) in Eq. (6) and (II) in Eq. (7), is often neglected in the absence of data for ${}_L R_{ij}$, $i \neq j$. Term (III), Eq. (8), and Eq. (9) contains the ordinary diffusion terms. Two extreme

cases can be identified from Eq. (6) through Eq. (9) if we neglect the turbulent shear correlation contribution term.

(i) Within a very short dispersive range, ${}_{L}R_{ii}(\tau)$ approaches unity for a very short time lag so that

$$\left.\begin{aligned} [X_1^2(t)] &= \tfrac{2}{3}\,\Gamma^2\,[u_{33}^2]t^3 + [u_{11}^2]t^2 \quad , \\ [X_2^2(t)] &= [u_{22}^2]t^2,\ [X_1(t)\ X_3(t)] = \Gamma[u_{33}^2]t^2, \text{ and} \\ [X_3^2(t)] &= [u_{33}^2]t^2 \quad . \end{aligned}\right\} \tag{10}$$

ii) For a long range dispersion, ${}_{L}R_{ii}(\tau)$ approaches a constant value, ${}_{i}T_{L}$, and ${}_{L}R_{ii}(\tau)$ approaches zero so that

$$\left.\begin{aligned} [X_1^2(t)] &\cong \tfrac{2}{3}\,\Gamma^2\,[u_{33}^2]\ {}_{3}T_{L}\ t^3 + [u_{11}^2]\ {}_{1}T_{L}\ t \quad , \\ [X_2^2(t)] &\cong 2\ [u_{22}^2]\ {}_{2}T_{L}\ t \quad , \\ [X_3^2(t)] &\cong 2\ [u_{33}^2]\ {}_{3}T_{L}\ t \quad , \text{ and} \\ [X_1(t)\ X_3(t)] &\cong \Gamma\ [u_{33}^2]\ {}_{3}T_{L}\ t^2 \quad . \end{aligned}\right\} \tag{11}$$

In particular, for asympotitic forms of the displacement measures, Corrsin (1959) reported that

$$\left.\begin{aligned} [X_1^2(t)] &\cong \tfrac{2}{3}\,\Gamma^2\,[u_{33}^2]\ {}_{3}T_{L}\ t^3 \quad , \text{ and} \\ [X_1(t)\ X_3(t)] &\cong \Gamma\ [u_{33}^2]\ {}_{3}T_{L}\ t^2 \end{aligned}\right\} \tag{12}$$

Batchelor (1949) showed that the time-dependent turbulent diffusivities could be related to the particle displacements as

$$K_{ij} = \tfrac{1}{2}\,\frac{d}{dt}\,[X_i\ X_j] = \tfrac{1}{2}\int_o^t [{}_{L}R_{ij}(\tau) + {}_{L}R_{ji}(\tau)]d\tau \tag{13}$$

if the distributions of x_i are jointly as well as separately normal. By examining the turbulent diffusion equation, Riley and Corrsin (1974)

showed that in a homogeneous turbulent flow with uniform shear, the eddy diffusivities differ formally from those for the diffusivities for an unsheared homogeneous flow. The eddy diffusivities in a sheared homogeneous shear flow are

$$K_{11}(t) = [u_{11}^2] \int_o^t {}_L R_{11}(\tau)d\tau + \Gamma\, [u_{11}^2]^{\frac{1}{2}}\, [u_{33}^2]^{\frac{1}{2}} \int_o^t \tau\, {}_L R_{13}(\tau)d\tau \ , \quad (14)$$

$$K_{13}(t) + K_{31}(t) = [u_{11}^2]^{\frac{1}{2}}\, [u_{33}^2]^{\frac{1}{2}} \int_o^t [{}_L R_{13}(\tau) + {}_L R_{31}(\tau)]d\tau + \Gamma\, [u_{33}^2] \int_o^t \tau\, R_{13}(\tau)d\tau \ , \quad (15)$$

$$K_{22}(t) = [u_{22}]^2 \int_o^t {}_L R_{22}(\tau)d\tau \ , \text{ and}$$

$$K_{33}(t) = [u_{33}]^2 \int_o^t {}_L R_{33}(\tau)d\tau \ . \quad (16)$$

2.2 RELATION BETWEEN LAGRANGIAN AUTOCORRELATION AND EULERIAN CORRELATION

The literature on the relation between Lagrangian autocorrelation and Eulerian correlation is quite vast. However, the available approaches for the estimation of the Lagrangian autocorrelation can be categorized into four groups based on their salient traits.

2.2.1 Linear-Correlation Method

In a homogeneous isotropic turbulence, the shape of the Lagrangian autocorrelation is proposed to be similar to either an axial Eulerian cross correlation (Mickelsen, 1955) or a single Eulerian autocorrelation (Gifford, 1955). Hay and Pasquill (1959) advanced the hypothesis and suggested that the Lagrangian correlation coefficient for a particle might decay with time in a similar manner to the Eulerian correlation coefficient measured at a fixed point, but with a different time scale, i.e.,

$$ {}_{L}R_{ii}(\xi) = {}_{E}R_{ii}(t) \quad \text{when} \quad \xi = \beta t \quad , \tag{17} $$

where β is the ratio of the Lagrangian to the Eulerian time scales, i.e., $\beta = {}_{L}T_{1}/{}_{E}T_{1}$.

Corrsin (1963) compared the shapes of Lagrangian and Eulerian spectra in the inertial subrange. By assuming that the total turbulent energy u^2 was identical in the Lagrangian and Eulerian system, he arrived at a theoretical prediction of β

$$ \beta = \frac{c}{i} \quad , $$

where c is a constant and i is the intensity of turbulence, $i = [u^2]^{\frac{1}{2}}/U$.

Direct estimations of both the Eulerian and Lagrangian spectra have been made by Gifford (1955). Using observations of floating balloons released from the meteorological tower at Brookhaven National Laboratory, an averaged value, $\beta \cong 3$, was found. Hay and Pasquill (1959) reported $\beta \cong 4$ from Mickelen's wind tunnel data. Based on monitoring the trajectories of tetroons at height of 2500 ft, Angell (1964) observed an average value near 3.3. Angell (1971) made further observations in the atmosphere near Las Vegas. β was found to have value about 3 and was inversely proportional to the turbulence intensity. Recent turbulence observations were made in the day time mixed layer near Boulder, Colorado. Hanna (1981) reported that β is about 1.7 and gave the formula $\beta = 0.7/i$.

2.2.2 Moving-Frame Autocorrelation Method

In the moving-frame autocorrelation approach the Lagrangian autocorrelation is estimated by the envelope of a set of Eulerian space-time cross correlations of the longitudinal fuctuating velocity under

the assumption of homogeneous and isotropic turbulence. This envelope, which connects the peaks of the cross correlations, is interpreted as a moving Eulerian autocorrelation which would be measured by a probe traveling steadily at the mean velocity. This scheme was put forward by Baldwin and Walsh (1961) and further explored by Balwin and Mickelson (1963). The advantage of this method is that it preserves the asymptotic value of Lagrangian autocorrelation function where the Lagrangian coefficient apparently approaches zero monotonically, but the Eulerian correlation dips below zero to slightly negative values before approaching a zero value asymptote. The shortcoming in principle of using the moving Eulerian autocorrelation as the Lagrangian autocorrelation, as quoted by Corrsin (1963), is that the Lagrangian velocity is effectively being approximated by sampling along an unknown random trajectory.

2.2.3 Probability Method

The probability method was based on Corrsin's (1959) "Independence hypothesis" and later modified by Johnson and Baldwin (1974). Corrsin proposed that the Lagrangian autocorrelation might be estimated from the general Eulerian space-time correlation by properly weighing the latter to account for fluid point distribution in space and time, i.e.,

$$ {}_{L}R_{11}(\tau) = \iiint_{V} W(x_i, \tau)\ {}_{E}R_{11}(x_i, \tau)dV \quad . \tag{18} $$

The weighting function, $W(x_i, \tau)$, is the probability of finding a fluid point injected at the origin in the region between x_i and $x_i + dx_i$ at any time τ.

Saffman (1963) assumed a functional form of an Eulerian spectral density, rather than an equivalent general Eulerian space-time correlation function. For lower turbulence intensity, β was reported to have a value of about $0.8/i$.

Philip (1963) employed a modified Gaussian function for the general Eulerian space-time correlation because it simplified the rather difficult computation which the independence hypothesis involved. The integral was solved in terms of a parameter which depends upon the Eulerian axial turbulent velocity, the Eulerian integral time and the longitudinal length scale.

2.2.4 Averaging Method

A relationship between the Lagrangian and Eulerian autocorrelations was proposed by Koper et al. (1978). The method is based on three novel trajectory, particle-space and reference-plane averges of Eulerian velocity products. The Lagrangian autocorrelation is approximated by a domain integral over all the usual Eulerian autocorrelations that are to be concurrently acquired within a flowfield. The Lagrangian-Eulerian autocorrelation may be expressed as

$$ {}_{L}R_{ij}(s, \tau) \cong \frac{1}{v} \int_{v} {}_{E}R_{ij}(x_k, \tau)dV \quad , \tag{19} $$

where s is the reference plane of the flowfield.

The variation of the resulting reference-point Lagrangian autocorrelation coefficient with increasing time delay is depicted in Figure 4 of Koper et al. (1979).

Notice that in a simplified case, the method coincides with the probability method stipulating a uniform weighting function. In an isotropic homogeneous turbulent flow the Eulerian autocorrelation is independent of its position and direction within the domain of the average flowfield. The method implies that ${}_{L}R_{1}(\tau) = {}_{E}R_{1}(\tau)$ with $\beta \cong 1.0$.

2.3 STOCHASTIC PROCESS OF PARTICLE MOTION

The Lagrangian approach to turbulent diffusion through a stochastic process was first introduced when Obukhov (1959) proposed that some problems of atmospheric diffusion may be represented by a Markov process. It is generally assumed in this method that the Lagrangian velocity of a fluid particle possesses a Markov process property in a homogeneous turbulent flow field so that

$$u(t + \tau) = \alpha(\tau)\, u(t) + n(t) \ , \tag{20}$$

where $n(t)$ satisfies $n = N(0, \sigma^2)$; σ^2 is the variance of u, i.e., $\sigma^2 = [u^2]$. $\alpha(\tau)$ was assumed to be ${}_{L}R_{11}(\tau)$ by Smith (1968). By assuming that the components of the velocities of particles in a given direction are normally distributed about the mean velocity component in the same direction, Jonas and Bartlett (1972) were also able to derive a similar form of Eq. (20). In addition, $\alpha(\tau)$ was also found to satisfy $\alpha(2\tau) = \alpha^2(\tau)$ and

$$\alpha(\tau) = \exp(-\tau/{}_{1}T_{L}) \ ,$$

which coincides with an exponential form of ${}_{L}R_{11}(\tau)$.

Langevin's equation may be derived from Eq. (20) by expanding, $u(t + \tau)$ in a Taylor form

$$\frac{d}{dt}\, u(t) + \beta'\, u(t) = \eta(t) \ . \tag{21}$$

Multiplying Eq. (21) by $u(t)$ and averaging produces

$$[\eta(t)\, u(t)] = [\beta'\, u^2(t)] \ . \tag{22}$$

In view of the Lagrangian form of the Navier-Stockes equation, the physical interpretation which emerges is that $[\eta(t)\, u(t)]$ is the statistical average of the rate of energy input to a fluid particle by

the pressure, while $[\beta' \; u^2(t)]$ is the viscous dissipation rate (Krasnoff and Peskin, 1971).

An analytical solution of Eq. (21) together with $u(t) = dx_1(t)/dt$ and boundary conditions, $x_1 = 0$ and $u(0) = u_o$ at $t = 0$, was presented by Gifford (1982). The mean-square displacement of fluid particles averaged over all values of u_o is

$$[X_1^2]_{u_o} = 2 \frac{[u^2]}{\beta'^2} (\beta t - 1 + e^{-\beta t}) \; . \tag{23}$$

If ${}_L R_{11}(\tau) = \exp(-\tau/{}_1T_L)$ is substituted into Eq. (3), the result of integration is exactly the same as Eq. (23) for $\beta' = {}_1T_L^{-1}$. The autocorrelation function calculated from Eq. (21) for zero initial velocity was found to be (Papulis, 1965)

$${}_L R_{11}(t,\tau) = \frac{[u(t + \tau) \; u \; (t)]}{[u^2]} = (1 - e^{-2\beta t}) e^{-\beta' \tau} \; . \tag{24}$$

This time-dependent function approaches the steady value $e^{-\beta\tau}$ only after diffusion times equal to several times the Lagrangian time scale ${}_1T_L$. The autocorrelation function calculated from Eq. (21) unconditioned by the initial velocity was also found by Papulis (1965)

$${}_L R_{11}(\tau) = e^{-\beta' |\tau|} \; . \tag{25}$$

Together they may imply that the popular exponential form of the Lagrangian autocorrelation is only applicable to very long range dispersion where the initial velocity can be considered as stationary. Equation (24) has a similar form to the coherence structure reported by Kristensen (1979), when the coherence loss due to eddy destruction is considered. The coincidence indicates that the Lagrangian autocorrelation may be best approximated by the moving Eulerian correlation method or the probability method for middle or long range diffusion.

Equation (20) with an exponential form of $\alpha_i(\tau)$ has been adopted by Reid (1979) for simulations of vertical dispersion in the neutral surface layer. Results were reported in good agreement with the available observation. Hanna (1979) compared Eq. (20) with observations in the planetary boundary layer. The linear relationship found in Eq. (20) was shown to be approximately valid and the magnitude of $\alpha_i(\tau)$ could be approximated by an exponential function to within $\cong$ 20 percent for the range of time lag from 1 sec to 60 sec. Note that the deviation of $\alpha_i(\tau)$ from the exponential function is more significant in the medium range of time delay.

Attempts have been made to take into account the behavior of the particles as they come into contact with the solid boundary as well as defining their motion in the nonhomogeneous flow above the surface. Both Hall (1975) and Durbin (1980) characterized the inhomogeneous turbulence by the spatial variable Lagrangian time scale. Numerical schemes have been proposed, yet further verification is needed.

3. APPROACH AND PROCEDURE

3.0 INTRODUCTION

The Baldwin and Johnson approach to the estimation of Lagrangian autocorrelation function is presented in Section 3.1. A brief block diagram of the numerical iterative scheme to calculate the Lagrangian autocorrelation is displayed. The diffusion equation employed in the research is shown in Section 3.2. A procedure for using a few anemometers located in the fixed Eulerian frame of reference to estimate the dispersion is discussed in Secton 3.3.

3.1 ESTIMATION OF LAGRANGIAN AUTOCORRELATION FUNCTION

A method for estimating the Lagrangian autocorrelation function from statistical measurements of the turbulent velocity in the fixed Eulerian frame of reference was proposed by Baldwin and Johnson (1972).

Lagrangian isotropy requires that the weighting function $W(x_i, \tau)$ in Eq. (2-18) exhibit spherical symmetry, and the experimental evidence shows it to be a Gaussian function (Frenkiel, 1953), i.e.,

$$W(r, \tau) = 2\pi[X_i^2(\tau)]^{-3/2} \exp\left[-\frac{r^2}{2[X_i^2(\tau)]}\right] . \tag{1}$$

Note that the coordinate system is a spherical one with its origin in the mean convective frame and

$$[X_1^2(\tau)] = [X_2^2(\tau)] = [X_3^2(\tau)] . \tag{2}$$

In an isotropic homogeneous turbulence, the spatial longitudinal velocity correlation, $f(r) = \overline{(u_1)_A (u_1)_B}/\overline{u^2}$, has the exponential form such that $f(r) = e^{-|r/L|}$, where point A and point B are separated with distance r along the longitudinal direction. By virture of the Karman-Howarth equation, $f(r) + r/2\ \partial f(r)/\partial r = g(r)$, the self consistent

lateral Eulerian space correlation, $g(r) = \overline{(u_2)_A\ (u_2)_B}/\overline{u^2}$, may be written as

$$ {}_E R_{22}(r, \theta, 0) = {}_E R_{33}(r, \theta, 0) = e^{-|r/L|}\ [1 - \tfrac{1}{2}\left|\tfrac{r}{L}\right|\ (1 - \cos^2\theta)]. \quad (3) $$

The Eulerian space-time correlation is assumed to have the functional form such that

$$ {}_E R_{ii}(r, \theta, \tau) = e^{-|r/L|}\ [1 - \tfrac{1}{2}\left|\tfrac{r}{L}\right|\ (1 - \cos^2\theta)] \cdot F(\tau/T_s)\ , \quad (4) $$

where $F(\tau/T_s)$ is an emperical formula for the convective Eulerian correlation.

The Lagrangian autocorrelation is found through iteration on Taylor's theorem and Corrsin's independence hypothesis, i.e., Eq. (2-1) and Eq. (2-18). By adopting the following non-dimensional variables,

$$ \xi = \frac{r}{L}\ ,\ t^* = \frac{\tau}{T_s} \quad \text{and} \quad \alpha = \frac{\sqrt{\overline{u'^2}}\ T_s}{L} \quad (5) $$

where T_s is the integral time scale of Eulerian space-time correlation and L is the integral Lagrangian scale, after some manipulation, the resulting equations are

$$ {}_L R_{11}(t^*) = F(t^*)\ \{e^{\alpha^2 I(t^*)}\ (1 - \operatorname{erf}\sqrt{\alpha^2 I(t^*)})\ [1 + 4\ \alpha^2 I(t^*) + \tfrac{4}{3}\ \alpha^4 I^2(t^*)] - \tfrac{2}{3}\sqrt{\frac{\alpha^2 I(t^*)}{\pi}}\ [5 + 2\alpha^2 I(t^*)]\} \quad (6) $$

and

$$ I(t^*) = \int_o^{t^*} \int_o^{t_1^*} {}_L R_{11}(t_2^*)\ dt_2^*\ dt_1^* \quad . \quad (7) $$

A numerical procedure was developed to solve Eq. (6) by iteration. The procedure was designed for various values of Eulerian diffusivity

parameter α. It assumes an exponential form of the Lagrangian autocorrelation,

$$_{L}R_{11}(t^*) = \exp(- A * \alpha * t^*) \quad . \tag{8}$$

The Lagrangian autocorrelation is determined by two variables, A and α. Where A is a function of the Eulerian diffusivity parameter and time.

A brief block diagram is presented in Table 1 to show the numerical iterative scheme.

3.2 DIFFUSION EQUATION

Considering the mass conservation of a control volume in fluid and neglecting the molecular diffusion, one obtains

$$\frac{\partial c}{\partial t} = - \nabla(Uc) \tag{9}$$

By Reynolds averaging and introducing the eddy diffusivity, $K_{ii} = uc'/\partial\bar{c}/\partial x_i$, the diffusion equation is obtained as

$$\frac{\partial \bar{c}}{\partial t} + U \frac{\partial \bar{c}}{\partial x_1} = \frac{\partial}{\partial x_1} (K_{11} \frac{\partial \bar{c}}{\partial x_1}) + \frac{\partial}{\partial x_2} (K_{22} \frac{\partial \bar{c}}{\partial x_2}) + \frac{\partial}{\partial x_3} (K_{33} \frac{\partial \bar{c}}{\partial x_3}) \tag{10}$$

In a uniform shear flow where $U = \Gamma x_3$, Eq. (10) was solved by Novikov (1958) with Eq. (2-11), (2-14), and (2-15) while assuming that the cross correlations, $R_{ij}(\tau)$, $i \neq j$, are negligible. The solution was presented in Monin and Yaglom (1971) for an absorbing boundary condition. We adapted it to a uniform shear flow, $U = \bar{U}(1 + \Gamma/\bar{U}\, x_3)$, i.e.,

$$\bar{c}(x_1, x_2, x_3, t) = \frac{1}{(4\pi t)^{3/2} \left[(K_{11} + \Gamma^2 k_{33}\, t^2/12)\, K_{22}\, K_{33}\right]^{1/2}}$$

$$\cdot \exp \left\{ - \frac{(x_1 - \bar{U}t - \Gamma x_3 t/2)^2}{4K_{11}t + \Gamma^2 K_{33} t^3/3} - \frac{x_2^2}{4K_{22}t} - \frac{x_3^2}{4K_{33}t} \right\} \quad . \tag{11}$$

For a continuous point source release, the differential equation becomes

$$U \frac{\partial \bar{c}}{\partial x_1} = \frac{\partial}{\partial x_1} (K_{11} \frac{\partial \bar{c}}{\partial x_1}) + \frac{\partial}{\partial x_2} (K_{22} \frac{\partial \bar{c}}{\partial x_2}) + \frac{\partial}{\partial x_3} (K_{33} \frac{\partial \bar{c}}{\partial x_3}) \quad . \quad (12)$$

The second term of longitudinal diffusion can be shown to be negligible as cited by Walters (1964).

The diffusion equation for a continuous line source in a uniform shear flow is

$$\bar{U} (1 + \frac{\Gamma x_3}{\bar{U}}) \frac{\partial \bar{c}}{\partial x_1} = \frac{\partial}{\partial x_3} (K_{33} \frac{\partial \bar{c}}{\partial x_3}) \quad .$$

By a simple transformation to a new inertial system of coordinates the solution presented by Roberts (unpublished, see Sutton (1953)) can be adopted for a ground release case,

$$\bar{c}(x_1, x_3) = \frac{3\ Q}{\Gamma\ \text{Gamma}(2/3)} [\frac{\Gamma}{9\ K_{33}\ x_1}]^{2/3} \exp[- \frac{\Gamma(x_3 + \frac{\bar{U}}{\Gamma})^3}{9\ K_{33}\ x_1}] \quad . \quad (13)$$

The solution stated above is subject to the following boundary conditions,

$$\begin{aligned} & K_{33} = \text{constant}, \\ & c \to 0 \quad \text{as} \quad x_1, x_2 \to \infty, \\ & c \to \infty \quad \text{at} \quad x_1 = x_3 = 0, \\ & K_{33} \frac{\partial c}{\partial x_3} \to 0 \quad \text{as} \quad x_3 \to 0 \ , \quad x_1 > 0, \text{ and} \\ & \int_o^\infty Uc(x_1, x_3)\, dx_3 = Q \ , \quad x_1 > 0. \end{aligned} \quad (14)$$

For an elevated line source, Smith's (1957) solution is employed for a uniform shear flow in this study, i.e.,

$$\bar{c}(x_1, x_3) = \frac{Q\,\bar{U}}{3\,K_{33}\,x_1\Gamma}\left(1 + \frac{x_3\Gamma}{\bar{U}}\right)^{1/2} \exp\left\{-\frac{\bar{U}^3\left(1 + \left(\frac{\Gamma x_3}{\bar{U}} + 1\right)^3\right)}{9\,\Gamma^2\,K_{33}\,x_1}\right\}$$

$$\cdot\, I_{-1/3}\left[\frac{2\,\bar{U}^3\left(1 + \frac{\Gamma x_3}{U}\right)^{3/2}}{9\,K_{33}\,x_2\,\Gamma^2}\right] . \qquad (15)$$

One notices that Eq. (15) has a similar form to the solution proposed by Lauwerier (1953), but it differs from Lauwerier's solution by a K_{33} term in the denominator and a modified Bessel function. A dimensional inconsistency was found in Lauwerier's analysis.

It is reasonable to assume a Gaussian distribution of the mean concentration field in the transverse cross-section since the diffusion equation contains only the single derivative with respect to x_2, $K_{22}\,\partial^2 c/\partial x_2^2$, with K_{22} independent of x_2. Hence

$$\bar{c}(x_1, x_2, x_3) \cong \frac{1}{\sqrt{2\pi}\,\sigma_2}\, e^{-\frac{x_2^2}{2\sigma_2^2}}\, \bar{c}(x_1, x_3)$$

i.e.,

$$\bar{c}(x_1, x_2, x_3) \cong \frac{Q\,\bar{U}\left(1 + \frac{x_3\Gamma}{\bar{U}}\right)^{1/2}}{3K_{33}x_1\Gamma(4\pi)^{1/2}\left(\frac{K_{22}\,x_1}{\bar{U}}\right)^{1/2}} \cdot I_{-1/3}\,\frac{2\,\bar{U}^3\left(1 + \frac{\Gamma x_3}{\bar{U}}\right)^{3/2}}{9\,K_{33}\,x_1\,\Gamma^2}$$

$$\cdot \exp\left(-\frac{x_2^2\,\bar{U}}{4\,K_{22}\,x_1} - \frac{\bar{U}\left(1 + \left(\frac{\Gamma x_3}{\bar{U}} + 1\right)^3\right)}{9\,\Gamma^2\,K_{33}\,x_1}\right) . \qquad (16)$$

It is interesting that $\bar{c}(x_1, x_2, x_3) \sim x_1^{-3/2} K_{22}^{-1/2} K_{33}^{-1} x_3^{1/2}$ agrees with Walters' (1965) asymptotical solution although a conjugate power law assumption was employed by Walters.

Huang (1979) proposed a non-Gaussian diffusion model for turbulent shear flow based on the statistical theory and K-theory. An analytic solution was presented based on Eq. (14) and the following conditions

$$U(x_3) = a\, x_3^p \quad ,$$

$$K_{33}(x_3) = b\, x_3^n \quad , \tag{17}$$

$$K_{33} = \frac{1}{2}\frac{d\sigma_2^2}{dt} = \frac{1}{2} U \frac{d\sigma_2^2}{dx_1} \quad ,$$

and the solution is

$$\bar{c}(x_1, x_2, x_3) = \frac{Q}{\sqrt{2\pi}\,\sigma_2} \exp\left[- \frac{(x_2 - x_{2s})^2}{2\sigma_2^2}\right] \frac{(x_3\, x_{3s})^{\frac{1-n}{2}}}{b\,\alpha\, x_1}$$

$$\cdot \exp\left[- \frac{a(x_3^\alpha + x_{3s}^\alpha)}{b\,\alpha^2\, x_1}\right] \cdot I_{-\nu}\left[\frac{2a(x_3\, x_{3s})^{\alpha/2}}{b\,\alpha^2\, x_1}\right] \quad . \tag{18}$$

Where x_{is} is the coordinate of the point source, and

$$\alpha = 2.0 + p - n \quad , \text{ and}$$

$$\nu = (1 - n)/\alpha \quad .$$

In a uniform shear flow with constant diffusivity, $n = 0$, $p = 0$, and $\sigma_2 = (2\, x_1\, k_{22}/U)^{1/2}$, Eq. (18) is identical to Eq. (16) as shown by a simple transformation of coordinates, where $x_{2s} = 0$ and $x_{3s} = \bar{U}/\Gamma$ were employed.

3.3 THE APPROACH

The statistical method in turbulent dispersion proposed in the present study is to apply estimates of the Lagrangian statistics to the Eulerian diffusion equation. As mentioned in Sec. 3.1, we are able to measure the Eulerian time scale, T_E, in the atmosphere and to calculate the Lagrangian time scale, ${}_iT_L$, by Baldwin and Johnson method with a specified Eulerian parameter, $\alpha = \sqrt{\bar{u}}\, T_3/\bar{U}^2 T_E$. T_s may be obtained from T_E if an universal functional form of the space-time correlation is recognized. From Eq. (2-14), (2-15) and (2-16) we are able to evaluate the asymptotic eddy diffusivities from the now known Lagrangian time scale. The dispersive quantities are then to be calculated from Eq. 16.

4. PRESENT DEVELOPMENTS

4.0 INTRODUCTION

The present analysis concentrated on obtaining basic information necessary to the approach and on verifying the approach under simplified conditions. It is intended to extend the method to a more general case for an inhomogeneous anisotropic flow field including middle range dispersion.

Section 4.1 describes the wind tunnel utilized in the present measurements. The velocity correlation measurements are presented in Section 4.2. Diffusion measurements under the same flow configuration are discussed in Section 4.3.

4.1 WIND TUNNEL

All the measurements were conducted in the Meteorological Wind Tunnel of the Fluid Dynamics and Diffusion Laboratory at Colorado State University. A detailed description of the Meteorological Wind Tunnel is given by Plate and Cermak (1963). Previous diffusion experiments performed in the Meteorological Wind Tunnel are summarized in Table 2 chronilogically. Measurements in this phase of the study were made in a neutrally stratified boundary layer. The test section begins at 40 ft downwind from the entrance of the wind tunnel. Table 3 shows the characteristics of the simulated atmospheric boundary layer in the wind tunnel. Homogenuity in the x_1 - x_2 plane is preserved in the simulated boundary. Figure 1 to Figure 3 show the mean velocity profiles and the local turbulent intensity profiles in the test section under different velocities. The effect of the lateral wall was examined as shown in Figure 4. The correlation measurements and the dispersion measurements

were performed within the range where the velocity deficit is no greater than 1 percent. The turbulent energy decay in the longitudinal direction is negligible.

4.2 CORRELATION MEASUREMENTS

Two single hot wires were employed in the velocity correlation measurements. Analog signals were recorded continuously by an AMPEX FR-1300 Recorder/Reproducer. The record and reproduce modules were carefully calibrated and a 2000 Hz low pass filter was used. A modified switch board was established so that two channels of data can be taken simultaneously. A SAICOR correlation and probability analyzer, model SAI-42, was employed for the data analysis. The SAI-42 correlator provides auto and cross correlation functions with incremental lag or time delay value ranging from 1 μ sec to 1 sec resulting in total time delays from 100 μ sec to 100 sec. Precomputation delay of 200 lag values selected in 50 lag increments allows the correlation function to be viewed symmetrically about zero or up to 200 lag values removed from zero (optionally to 2000 points). The averaging is accomplished digitally with fixed summation ranging from 2^9 to 2^{17} in binary steps. The correlation function was displayed on a X-Y recorder in the form of 100 discrete points. A schematic diagram of the experimental set up is shown in Table 4. Data were continuously recorded by the AMPEX recorder for 5 minutes. Auto, space, and space-time correlation functions were obtained during the measurements. The space correlation functions in the x_3 direction were measured in the upward direction. The space correlation functions in the x_1-, x_2-, and x_3-directions at $x_{1s} = 0$ cm, $x_{3s} = 10$ cm, and $U_\infty = 200$ cm/sec are displayed in Figure 5 through Figure 7, respectively. Figure 8 through Figure 10 shows the space

correlation functions at x_{1s} = 0 cm, x_{3s} = 20 cm, and U_∞ = 200 cm/sec in the x_1-, x_2-, and x_3-directions respectively. The longitudinal autocorrelation functions at x_{3s} = 10 cm and x_{3s} = 20 cm are shown in Figure 11. As cited by Comte-Bellot and Corrsin (1971), the upstream probe imposes a wake effect on the downstream probe. Although the two probes have been placed such that two wires are perpendicular to each other, the wake effect of the upstream probe is still significant. Figure 12 shows the effect by spacing the downstream probe with Δx_2 away from the stream-wise direction. Hence, both space and space-time correlation functions are subject to an error which reduces the value at short separation in the longitudinal direction. The space correlations shown in Figure 5 and Figure 8 were under the upstream wake effect for short separations. The space-time correlation functions with longitudinal separation, $R_{11}(\Delta x_1, 0, x_{3s}, t_o + \Delta x_1/U)$, was constructed by forming the envelope of the maximum cross correlations, with optimum delay time $T_m \cong \Delta x_1/U$, of two simultaneously recorded hot-wire signals with separation Δx_1. The resulting space-time correlation functions, extrapolated to Δx_2 = 0, are displayed in Figure 13 and Figure 14 for x_{3s} = 10 cm and x_{3s} = 20 cm respectively. The integral time scale of the space-time correlation was found to increase as the height increases. The space-time correlation functions measured in the simulated atmospheric boundary layer were compared with previous measurements in a uniform flow downwind from a mesh grid. Figure 15 shows that the normalized space-time correlation are in good agreement with Comte-Bellot and Corrsin (1971). This seems to support the contention that a universal functional form of the space-time correlation may be applicable to the atmospheric boundary. It is also implied that the

homogenuity assumption is adequate to the atmospheric boundary layer on a horizontal plane. And the inhomogenuity of the atmospheric boundary layer may be characterized by the time scale of the space-time correlation which is a function of x_3.

The Lagrangian autocorrelation was obtained in the numerical iteration scheme as described in Section 3.1. Table 5 shows the integral scale of the Lagrangian autocorrelation in terms of the space-time integral time scale compared with different Eulerian space-time correlation models. The Eulerian time scale ratio, T_s/T_E, was plotted in Figure 16 versus the Eulerian parameter, α/i, with different models employed for the independent hypothesis, where i denotes the local turbulent intensity. Figure 17 shows the Lagrangian scale as a function of the Eulerian parameter, α. Although the data presented here are not sufficient to reach a definite conclusion, one might suggest that a general functional form of the Eulerian space-time correlation function is applicable to the atmospheric boundary layer.

4.3 Diffusion Measurements

Ethane was released from a 0.95 cm diameter port as the tracer gas. The tracer gas was released at a concentration of 10 percent ethane at a flow rate of 36.75 cc/sec. The density of the ethane mixture was balanced to be the same as the air density by adding nitrogen and carbon-dioxide. After the release of the tracer gas began, the sample collection system was flushed several times. A final sample was drawn over a period of approximately 3 minutes and held for subsequent analysis. Once samples were isolated within the collection system, the tracer gas flows were terminated to prevent background buildup in the wind tunnel.

A total of 42 samples were collected per run; two of them are the background concentrations in the wind tunnel. These samples were taken on the lateral x_2-x_3 plane downwind from the point source. Three release heights (ground, x_{3s} = 10 cm, and x_{3s} = 20 cm) for the point source were employed at two different wind speeds (U_∞ = 200 cm/sec and U_∞ = 300 cm/sec). Samples were taken at x_1 = 100, 200, and 500 cm downwind from the point source.

A Hewlett-Packard 5700 A gas chromatograph with a flame ionization detector was utilized to analyze the samples. A detailed description of the gas chromatograph may be found in Allwine, Meroney and Peterka (1979). The analog output from the gas chromatograph was converted to a digital signal using a HP-3380 Integrator. Further information about the integrator was given by Petersen and Cermak (1980).

The background concentration was subtracted from each sampled concentration. Only the data for U_∞ = 200 cm/sec and the elevated source releases are presented in the present study in accordance with the statistical measurements in the turbulence field.

The observed dispersion data were compared with the analytical prediction of Eq. (3-16) and Eq. (3-18) and are included in Table 6 through Table 17. The distance x_1 = 100, 200, and 500 cm downwind from the point source are considered as the distances of short-middle, middle, and long range dispersion respectively.

Table 6 through Table 8 display the dispersion data in the anisotropic homogeneous uniform shear flow, where the uniform shear is the value measured at the point source height x_{3s} = 10 cm. The data are very much distorted from the prediction for short range dispersion. (Table 5, (b) Eq. (3-16) with constant diffusivity in the x_i-direction,

(c) Eq. (3-18) with constant diffusivity in the x_i-direction, (d) Eq. (3-18) with constant diffusivity in the x_i-, x_2-direction and linear varying diffusivity in the x_3-direction). The error is obvious since the asymptotic Lagrangian time scale is not entirely applicable to the short range dispersion. Although the theory is not completely applicable at this range, an interesting result was found that the ${}_{11}T_L$ at x_{3s}= 20 cm is twice the value of ${}_{11}T_L$ at x_{3s} = 10 cm. This leads to a simple assumption that the vertical eddy diffusivity varies linearly with the height x_3. The result is then compared with the observed dispersion data in the (d) part of Table 6 through Table 17.

Table 9 through Table 11 shows the dispersion data in the isotropic homogeneous uniform shear flow, where the uniform shear is the value measured at the point source height x_{3s} = 10 cm. Although the analytical solutions still deviate from the observed data the lateral spread of the plume is much better predicted by the isotropic homogeneous approach than the anisotropic homogeneous approach.

In general, the analytical solution produces better results for long-range dispersion and higher elevated point source release. Equation (3-16) predicts better for the high elevated source release, since the constant shear assumption is better approximated. The ground concentrations were predicted within 10 percent error by Eq. (3-18) with linearly varying diffusivity in the vertical direction for long-range dispersion and the high elevated point source release (as seen in Table 17).

5. SUMMARY AND FURTHER DEVELOPMENT

5.1 SUMMARY

The purpose of this research is to examine the Baldwin and Johnson approach and to establish a practical predictive scheme for the atmospheric dispersion at a nuclear reactor site. Data analyzed in the present study expose the problems involved. The evaluation process is not complete; nevertheless, some conclusions are possible.

- Failure to predict short range dispersion in the present study is clear, but expected because the longitudinal diffusion term was neglected in the diffusion equation. Furthermore, the Lagrangian statistics applied in the current equations are developed for the asymptotic case only. The Lagrangian statistics are overestimated when applied to the short range dispersion. The measurements expose the error involved when one uses an asymptotic solution of the diffusion equation for the analysis of the short range and middle range dispersion.
- Although in the literature of statistical turbulence the travel time of a particle equal to 10 T_L is considered as a long-range diffusion, it was found inappropriate in the present study. The distance $x = 200$ cm is about 11 times the Lagrangian time scale carried by the local mean wind, yet the dispersion data deviate from the assymptotic estimates by a significant amount. It is necessary to determine more specifically the range over which the assymptotic diffusion equation is valid and the error involved at closer distances.
- A modified varying vertical diffusivity approach provided a better comparison with the diffusion data than the constant

eddy diffusivity assumption. This supports the idea that an approach based on the plane-wise homogeneous assumption may be appropriate in the atmospheric diffusion if certain modifications were made. Just because the Lagrangian statistics are simplified, the conclusion should not be made that an isotropic turbulence approach is better than an anisotropic turbulence approach. It is also necessary to have more information on the relation between eddy diffusivity and the spatial coordinates. This may be achieved through further investigation of the space-time correlations in the wind tunnel.

- The normalized longitudinal space-time correlation measured in the simulated boundary layer implies self-preservation exists despite the variation of height. If more information about the longitudinal space-time correlation with transverse separations can be obtained, the Lagrangian autocorrelation in the inhomogeneous flow field may be obtained from the independent hypothesis with some modification.
- Since eddy destruction tends to reduce the coherence structure in a turbulent flow field, the exponential form of the Lagrangian autocorrelation is no longer adequate for a middle range dispersion study. The asymptotic form of the eddy diffusivity should not be used. A further study of the middle range dispersion is necessary. Perhaps the autocorrelation function derived by Papulis (1965) as Equation (2-24) is appropriate for middle range dispersion.
- In general, the Baldwin and Johnson approach provides a fair comparison to measurements. It predicts the long-range

dispersion within the error of $\cong$ 40 percent under some simplified assumptions. It is expected even with such simplification that the predicted data will be more accurate if dispersion data were compared at longer distance downwind from the elevated point source. Hence, the approach should improve its predictions capabilities in subsequent evaluations when the simplifying assumptions are removed.

5.2 FURTHER DEVELOPMENT

Further investigation of this research is concentrated on the modification of the Baldwin and Johnson approach. Based on the summary described in Sec. 5.1, the following aspects are desired in further study.

- A complete description of the longitudinal space-time correlation function in the vertical direction is necessary to extend the functional form of the normalized space-time correlation to the inhomogeneous flow. The inhomogeneity is then characterized by the vertically varying eddy diffusivity through the space-time correlation.
- The exponential form of the Lagrangian autocorrelation function and Eq. (2-24) need to be examined since better prediction of the horizontal plume standard deviation are reported based on Eq. (2-24). (See Gifford, 1982).
- In order to include the middle range dispersion, modification on the program EULLAG is necessary to calculate the first integral of the Lagrangian autocorrelation function for $t \leqq {}_1T_L$.

- Diffusion measurements should be extended to the largest distance which can be reached in the wind tunnel for a better asympotical diffusion simulation.

REFERENCES

Allwine, K. J., Meroney, R. N., and Peterka, J. A., "Rancho Seco building wake effects on atmospheric diffusion: simulation in a meteorological wind tunnel," CER77-78KJA-RNM-JAP25, Colorado State University, 1979.

Angell, J. K., "Measurements of Lagrangian and Eulerian properties of turbulence at a height of 2500 ft," Quart. J. Roy. Meteo. Soc., Vol. 90, pp. 50-71, 1964.

Angell, J. K., "Lagrangian-Eulerian time scale ratios estimated from constant volume balloon flights past a tall tower," Quart. J. Roy. Meteo. Soc., Vol. 97, pp. 87-92, 1971.

Baldwin, L. V. and Walsh, T. J., "Turbulent diffusion in the core of fully developed pipe flow," A.I.Ch.E. J., Vol. 7, No. 1, pp. 53-61, 1961.

Baldwin, L. V. and Michelsen, W. R., "Turbulent diffusion and anemometer measurements," American Soc. of Civil Engineers Transactions, Vol. 128, No. 1, pp. 1595-1626, 1963.

Baldwin, L. V. and Johnson, G. R., "The estimation of turbulent diffusivities from anemometer measurements. Part I: Fluid particles. Colorado State University, Civil Engineering Paper CEP71-72LVB-GRJ42, 1972.

Batchelor, G. K., "Diffusion in a field of homgeneous turbulence," Aust. J. Sci. Rec. Ser. A, Vol. 2, pp. 437-450, 1949.

Comte-Bellot, G. and Corrsin, S., "Simple Eulerian time correlation of full- and narrow-band velocity signals in grid-generated "isotropic" turbulence," J. Fluid Mech., Vol. 18, Part 2, pp. 273-337, 1971.

Corrsin, S., "Remarks on turbulent heat transfer," Proc. of the Iowa Thermodynamics Symposium, University of Iowa, Iowa City, pp. 5-30, 1953.

Corrsin, S., "Progress report on some turbulent diffusion research," Adv. Geophys., Vol. 6, pp. 161-164, 1959.

Corrsin, S., "Estimates of the relation between Eulerian and Lagrangian scales in large Reynolds number turbulence," J. Atmos. Sic., Vol. 20, pp. 115-119, 1963.

Corrsin, S., "Discussion on turbulence measurements," American Soc. of Civil Engineers Transactions, Vol. 128, No. 1, pp. 1627-1631, 1963.

Counihan, J., "Adiabatic atmospheric boundary layer: A review and analysis of data from the period 1880-1972," Atmos. Environ., Vol. 19, pp. 871-905, 1975.

Durbin, P. A., "A random flight model of inhomogeneous turbulent dispersion," Phys. Fluids, Vol. 23, No. 11, pp. 2151-2153, 1980.

Farve, A. J., "Review of space-time correlations in turbulent fluids," Trans. ASME, J. Applied Mech., Vol. 32, pp. 241-257, 1965.

Frenkiel, F. N., "Turbulent diffusion: mean concentration distribution in a flow field of homogeneous turbulence," Advances in Applied Mech., Vol. 3, Mises and von Karman (editors), Academic Press, Inc., pp. 61-107, 1953.

Frenkiel, F. N. and Klebanoff, P. S., "Space-time correlations in turbulence," Dynamics of Fluids and Plasmas (ed., S. I. Pai), Academic Press, pp. 257-274, 1966.

Gifford, F. A., "A simultaneous Lagrangian-Eulerian turbulent experiment," Mon. Wea. Rev., Vol. 83, pp. 293-301, 1955.

Gifford, F. A., "Horizontal diffusion in the atmosphere: A Lagrangian-dynamical theory," Atmos. Environ., Vol. 16, No. 3, pp. 505-512, 1982.

Gifford, F. A., "Long-range plume dispersion: comparisons of the MT. ISA data with theoretical and empirical formulas," Atmos. Environ., Vol. 16, No. 6, pp. 1583-1586, 1982.

Hall, C. D., "The simulation of particle motion in the atmosphere by a numerical random-walk model," Quart. J. R. Met. Soc., Vol. 101, pp. 235-244, 1975.

Hanna, S. R., "Some statistics of Lagrangian and Eulerian wind fluctuations," J. of Appl. Meteoro., Vol. 18, pp. 518-525, 1979.

Hanna, S. R., "Lagrangian and Eulerian time-scale relations in the daytime boundary layer," J. of App. Met., Vol. 20, pp. 242-249, 1981.

Hay, J. S. and Pasquill, F., "Diffusion from a continuous source in relation to the spectrum and scale of turbulence," Adv. in Geophys., Vol. 6, pp. 345-365, 1959.

Huang, C. H., "A theory of dispersionin turbulent shear flow," Atmos. Environ., Vol. 18, pp. 453-463, 1979.

Jonas, P. R. and Bartlett, J. T., "The numerical simulation of particle motion in a homogeneous field of turbulence," J. Comp. Phys., Vol. 9, pp. 290-302, 1972.

Koper, C. A., Jr., and Sadeh, W. Z., "Investigation of turbulent diffusion in the extreme lower atmosphere," Fourth Symposium on Turbulence, Diffusion and Air Pollution, Jan. 15-18, pp. 665-672, 1979.

Koper, J. C. A., Sadeh, W. Z., and Turner, R. E., "A relation between the Lagrangian and Eulerian turbulent velocity autocorrelations," AIAA J., Vol. 16, No. 9, pp. 969-975, 1978.

Krasnoff, E. and Peskin, R. L., "The Langevin model for turbulent diffusion," Geophs. Fl. Dyns., Vol. 2, pp. 123-146, 1971.

Kristensen, L., "On longitudinal spectral coherence," Boundary-Layer Meteoro., Vol 16, pp. 145-153, 1979.

Lauwerier, H. A., "Diffusion from a source in a skew velocity field," Appl. Sci. Res., Vol. A4, pp. 153-156, 1953.

Mickelsen, W. R., "An experimental comparison of the Lagrangian and Eulerian correlation coefficients in homogeneous isotropic turbulence," NACA TN 3570, 1955.

Monin, A. S. and Yaglorn, A. M., "Statistical Fluid Mechanics: Mechanics of Turbulence, Volume 1," MIT Press, 1971.

Papoulis, A., "Probability, Random Variable, and Stochastic Processes," McGraw-Hill, New York, 1965.

Petersen, R. L., Cermak, J. A., and Hisato, M., "ASARCO stable nighttime condition fluid modeling investigation," CER79-80RLP-JEC-MH58, Colorado State University, 1980.

Philip, J. R., "Relations between Eulerian and Lagrangian Statistics," Phys. Fluids Supplement, Vol. 10, Part II, S69-71, 1967.

Plate, E. J. and Cermak, J. E., "Micrometeorological wind tunnel facility, description and characteristics," CER63EJP-JEC9, Colorado State University, 1963.

Reid, J. D., "Markov chain simulations of vertical dispersion in the neutral surface layer for surface and elevated release," Boundary-Layer Meteoro., Vol. 16, pp. 3-22, 1979.

Riley, J. J. and Corrsin, S., "The relation of turbulent diffusivities to Lagrangian velocity statistics for the simplest shear flow," J. of Geophs., Vol. 79, No. 12, pp. 1768-1771, 1974.

Saffman, P. G., "An approximate calculation of Lagrangian autocorrelation for stationary homogeneous turbulence," J. Appl. Sci. Res., Vol. 11, pp. 245-255, 1963.

Smith, F. B., "The diffusion of smoke from a continuous elevated point-source into a turbulent atmosphere," J. of Fluid Mechanics, Vol. 2, pp. 49-76, 1957.

Smith, F. B., "Conditioned particle motion in a homogeneous turbulent field," Atmos. Environ., Vol. 2, pp. 491-508, 1968.

Sutton, O. G., "Micrometeorology," New York, McGraw-Hill, 1953.

Taylor, G. I., "Diffusion by continuous movements," Proc. London Math. Soc. (2), 20, pp. 196-212, 1921.

Walters, T. S., "The effect of diffusion in the mean wind direction in atmospheric turbulence," Mathematika, Vol. 11, pp. 119-124, 1964.

Walters, T. S., "Diffusion from an elevated point source into a turbulent atmosphere," Mathematika, Vol. 12, pp. 49-57, 1965.

TABLES

TABLE 1
A computational numerical scheme of calculating the Lagrangian autocorrelation function (program EULLAG).

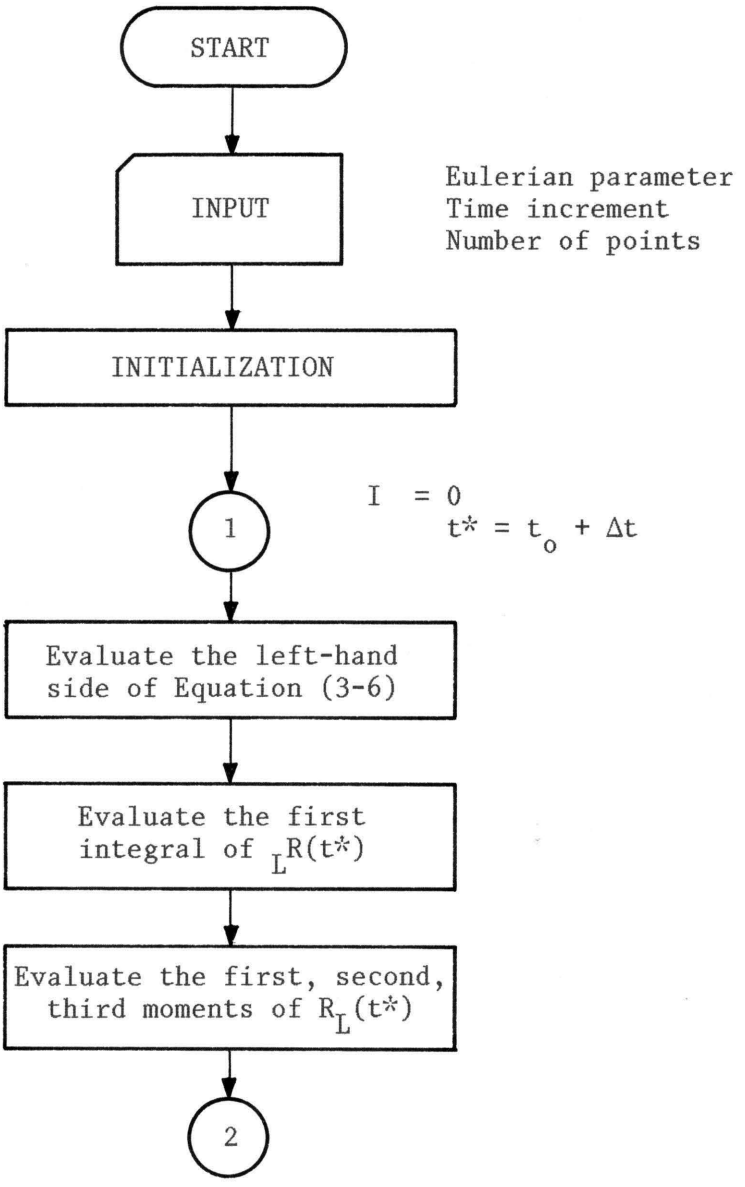

Table 1 (continued)

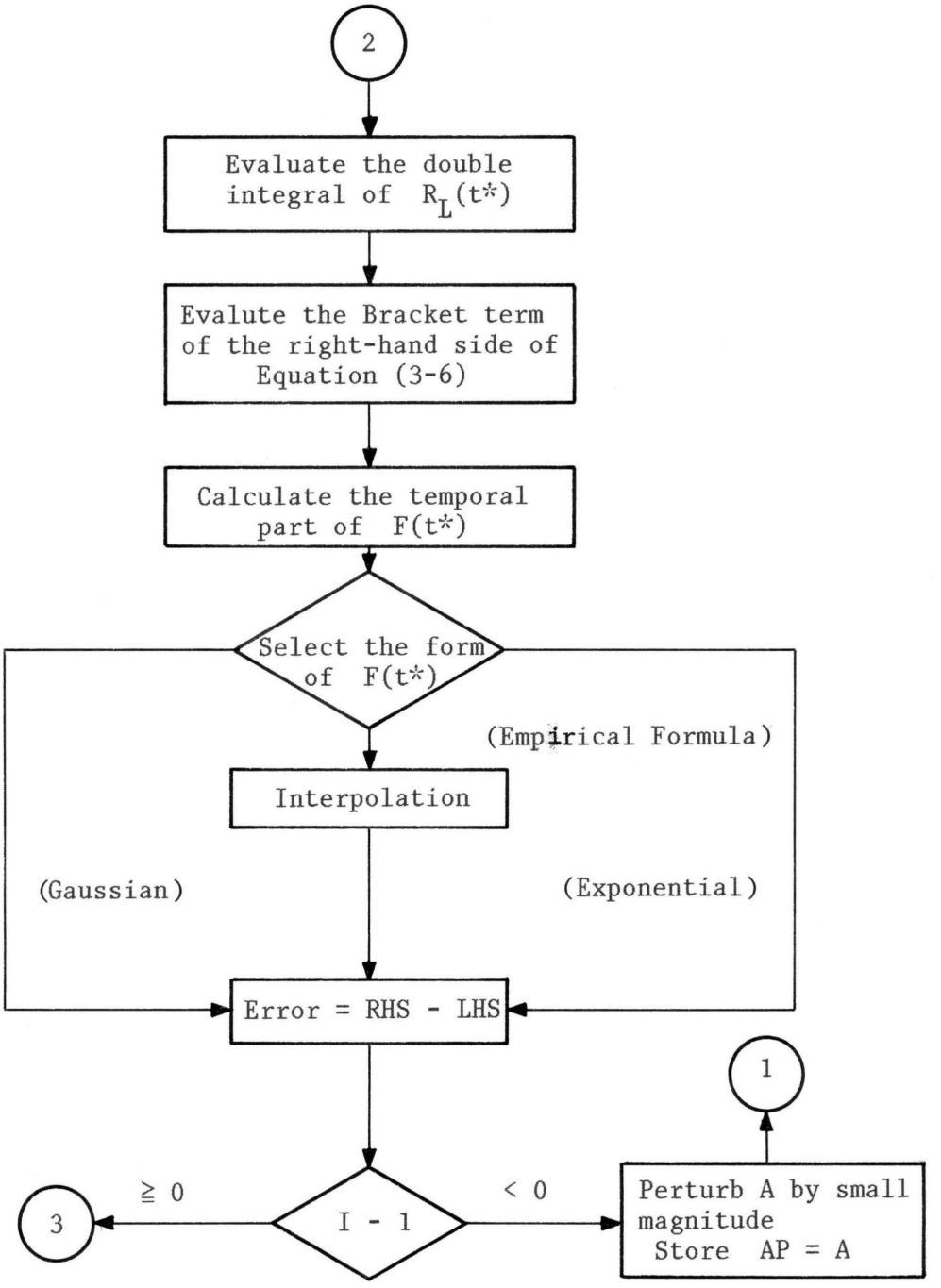

Table 1 (continued)

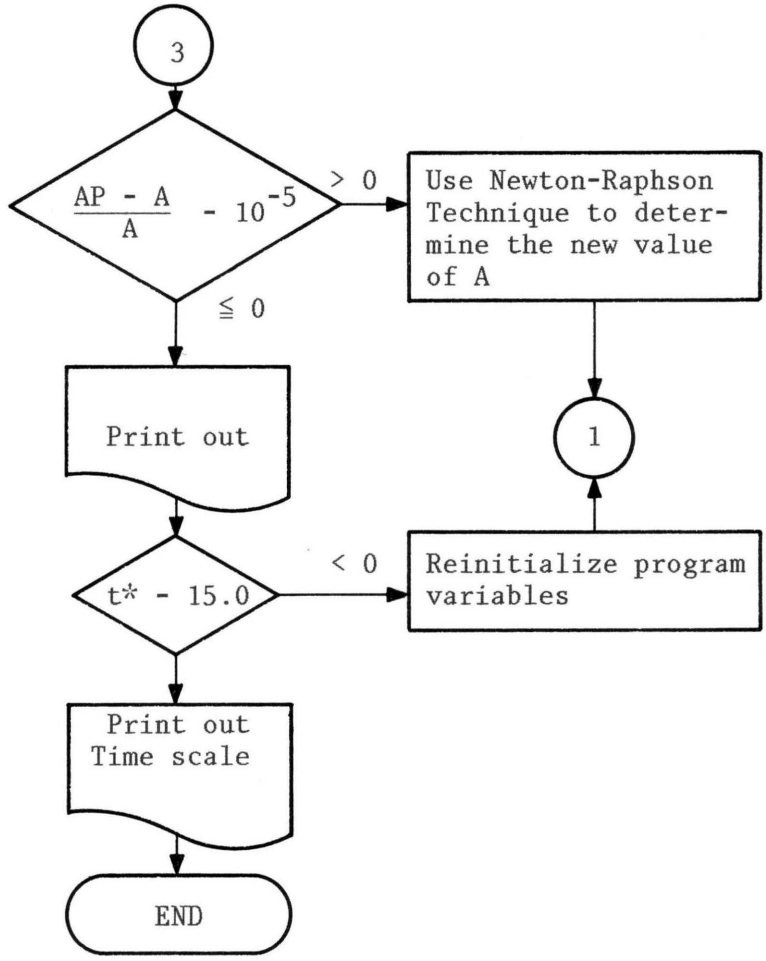

TABLE 2
Summary of previous diffusion measurements conducted in the Meteorological Wind Tunnel

EXPERIMENTS REPORTED BY: (Year)	WIND TUNNEL TEST SECTION AND TYPE	TYPE AND POSITION OF THE SOURCE	HEIGHT AND TYPE OF RELEASE	MAXIMUM SAMPLING DISTANCE	NATURE OF SURFACE	STRATIFICATION	TRACER	DIFFUSION MEASUREMENTS	U_*, Z_o, U_∞, δ, n	TURBULENT INTENSITY	SPECTRUM AUTO-CORRELATION
K. S. Davar (1961)	6' x 6' x 28' Recirculating	Point Source X_o = 6'	Ground and elevated Continuous	7'	Smooth Aluminum	Neutral	Anhydrous Ammonia	Complete mapping of concentration field	δ=12.1 cm/s U_∞=183 cm/s	$\sqrt{\overline{u'^2}}$, $\sqrt{\overline{v'^2}}$, $\sqrt{\overline{w'^2}}$	No
M. Foreh (1961)	8' x 8' x 80' Open Circuit (MWT)	Line Source X_o = 15.5' 33.5'	Ground Continuous	21' 43.5'	Smooth	Neutral	Anhydrous Ammonia	Vertical concentration profiles	n=0.143 U_∞=274 cm/s 365 cm/s 488 cm/s	$\sqrt{\overline{u'^2}}$, $\sqrt{\overline{v'^2}}$	Yes
R. C. Malhotra (1962)	6' x 6' x 28' Recirculating	Point Source X_o = 6'	Ground Continuous	7.5'	Smooth Aluminum	Neutral and Unstable	Anhydrous Ammonia	Complete mapping of concentration field		No	No
A. A. Quraishi (1963)	6' x 6' x 80' Open Circuit	Line Source X_o = 46'	Ground and elevated Continuous	12'	Plastic Roughness elements on wooden planks	Neutral	Anhydrous Ammonia	Vertical concentration profiles	δ=50 cm/s U_*=56.1 cm/s U_∞=609 cm/s	$\sqrt{\overline{u'^2}}$, $\sqrt{\overline{v'^2}}$, $\overline{uv}$	Yes
S. Bhaduri (1963)	6' x 6' x 28'	Point Source X_o = 6'	Ground and elevated Continuous	6.5'	2-D Roughness elements ¼" HT., 3" Apart	Neutral	Anhydrous Ammonia	Complete mapping of concentration field	U_∞ = 274 cm/s n =0.34 U_* varies with $\frac{x}{\delta}$ (Fig. 17)	$\sqrt{\overline{u'^2}}$, $\overline{uw}$	Yes
D. Kesic (1967)	6' x 6' x 28' Recirculating	Point Source X_o = 27'	Elevated Instantaneous	5"	Smooth Wooden	Neutral	Heat	Axial vertical and horizontal temperature profiles		$\overline{u^2}$, $\overline{v^2}$, $\overline{uv}$	No
M. Yang (1966)	6' x 6' x 80' Recirculating (MWT)	Point Source X_o =40', 55' 65'	Ground and elevated Continuous	20"	Pegs	Neutral Unstable Stable	Pure Helium	Axial vertical and horizontal temperature profile			No
S. Koehler (1967)	6' x 6' x 80' Recirculating (MWT)	Point Source X_o = 65'	Ground and Continuous	10'	Smooth Aluminum	Stable	Pure Helium	Vertical and ground level concentration profiles	n=0.143 Z_o =0.0028 m U^∞=609 cm/s U_* = $x^{-0.14}$		No
C. Shih (1966)	6' x 6' x 80' Recirculating (MWT)	Point Source X =2',7', 15',20',40', 60'	Ground Continuous	15'	Smooth Wooden and Aluminum	Neutral	Pure Helium	Free stream roughness changed	U_∞ =213 cm/s U_* =0.3 X $\sqrt{0.0287}$ Z_o =0.141 ν/U_*		No
S. Chandra (1967)	6' x 6' x 80' Recirculating (MWT)	Point Source 24' from aluminum	Elevated 8' Instantaneous	4'	Smooth	Neutral	Pure Helium	Complete mapping	U_∞ = 609 cm/s δ = 40 cm	$\sqrt{\overline{u'^2}}$, $\sqrt{\overline{w'^2}}$	Yes
B. T. Yang (1972)	6' x 6' x 80' Recirculating (MWT)	Point Source X_o = 11 m	Ground Instantaneous Continuous	5.5 m	Smooth Aluminum	Neutral	Laser Light	Continuous source complete mapping at X = 4 m	U_* =5.82 cm/s Z_o =0.94 X 10^{-3} cm U^∞ =117 cm/s n = 0.14 δ =28 cm	$\sqrt{\overline{u'^2}}/U = \left(\frac{Z}{\delta}\right)^{-0.42}$	No
F. H. Chaudhry (1969)	6' x 6' x 80' Recirculating (MWT)	Point Source X_o = 65'	Ground and Elevated Continuous		Smooth Aluminum	Neutral Stable	K-85	Complete mapping	U_* =12.37 cm/s Z_o =2.44 x 10^{-3} cm U^∞ =300 cm/s δ =73.152 cm	$\sqrt{\overline{u'^2}}$, $\sqrt{\overline{v'^2}}$, $\sqrt{\overline{w'^2}}$, $\sqrt{\overline{t'^2}}$, $\overline{u'w'}$	No
R. V. Hatcher (1977)	6' x 6' x 80' Recirculating (MWT)	Point Source	Ground and Elevated Continuous	8 m	Smooth	Neutral Stable	Ethane Propane	Complete discrete data in space (All run number 9)	n =0.144 U_∞ =232 cm δ =120 cm U_* =11.06 cm/s Z_o =0.02034 cm	No	No
Present Study (1981)	6' x 6' x 80' Recirculating (MWT)	Point Source X_o = 13 m	Ground and Elevated Continuous	8 m	Smooth	Neutral Stable	Ethane	Complete mapping of concentration field	n =0.166 U_* =7.25 cm/s Z_o =4 x 10^{-3}cm U^∞ =200 cm/s δ =45 cm	$\sqrt{\overline{u'^2}}$	Yes
									n =0.163 U_* =12.9 cm/s Z_o =2 x 10^{-3}cm δ =45 cm U_∞ =300 cm/s	n =0.146 U_* =21.7 cm/s Z_o =1 x 10^{-3} cm δ =45 cm U_∞ =500 cm/s	

TABLE 3
Characteristics of the simulated atmospheric boundary layer

Fixed Z_o Scale Ratio: .45/600	MODEL SCALE (1/1250)			PROTOTYPE			FIELD RESULT COUNIHAN (1975)		
	U_∞ = 2 m/s U_* = 0.0725 m/s	U_∞ = 3 m/s U_* = 0.129 m/s	U_∞ = 5 m/s U_* = 0.217 m/s	U_∞ = 2 m/s U_* = 0.0725 m/s	U_∞ = 3 m/s U_* = 0.0129 m/s	U_∞ = 5 m/s U_* = 0.217 m/s	U_∞ - 2 m/s U_* = 0.0725 m/s	U_∞ = 3 m/s U_* = 0.0129 m/s	U_∞ = 5 m/s U_* = 0.217 m/s
δ (m)	0.45	0.45	0.45	600	600	600	600	600	600
n	0.166	0.163	0.146	0.166	0.163	0.146	0.14	0.13	0.12
Z_o (m)	4.0×10^{-5}	2.0×10^{-5}	1.0×10^{-5}	0.05	0.025	0.0125	0.05	0.025	0.0125
$\left(\frac{U_*}{U_\infty}\right)^2$	1.314×10^{-3}	1.85×10^{-3}	1.88×10^{-3}	1.314×10^{-3}	1.85×10^{-3}	1.88×10^{-3}	1.97×10^{-3}	1.79×10^{-3}	1.61×10^{-3}
$\left(\frac{\sqrt{\overline{u'^2}}}{U}\right)_{z/\delta = 1/20}$	0.125	0.155	0.120	0.125	0.155	0.120	0.155	0.140	0.128
$\left(\frac{\sqrt{\overline{u'^2}}}{U}\right)_{z/\delta = 1/6}$	0.10	0.106	0.085	0.10	0.106	0.085	0.131	0.120	0.111
Λ_L (m) $\left(z/\delta = 0.444\right)$	0.103	0.17		129.1	212.5		220 (approx.)	250 (approx.)	

TABLE 4
Aparatus set up for velocity correlation measurements

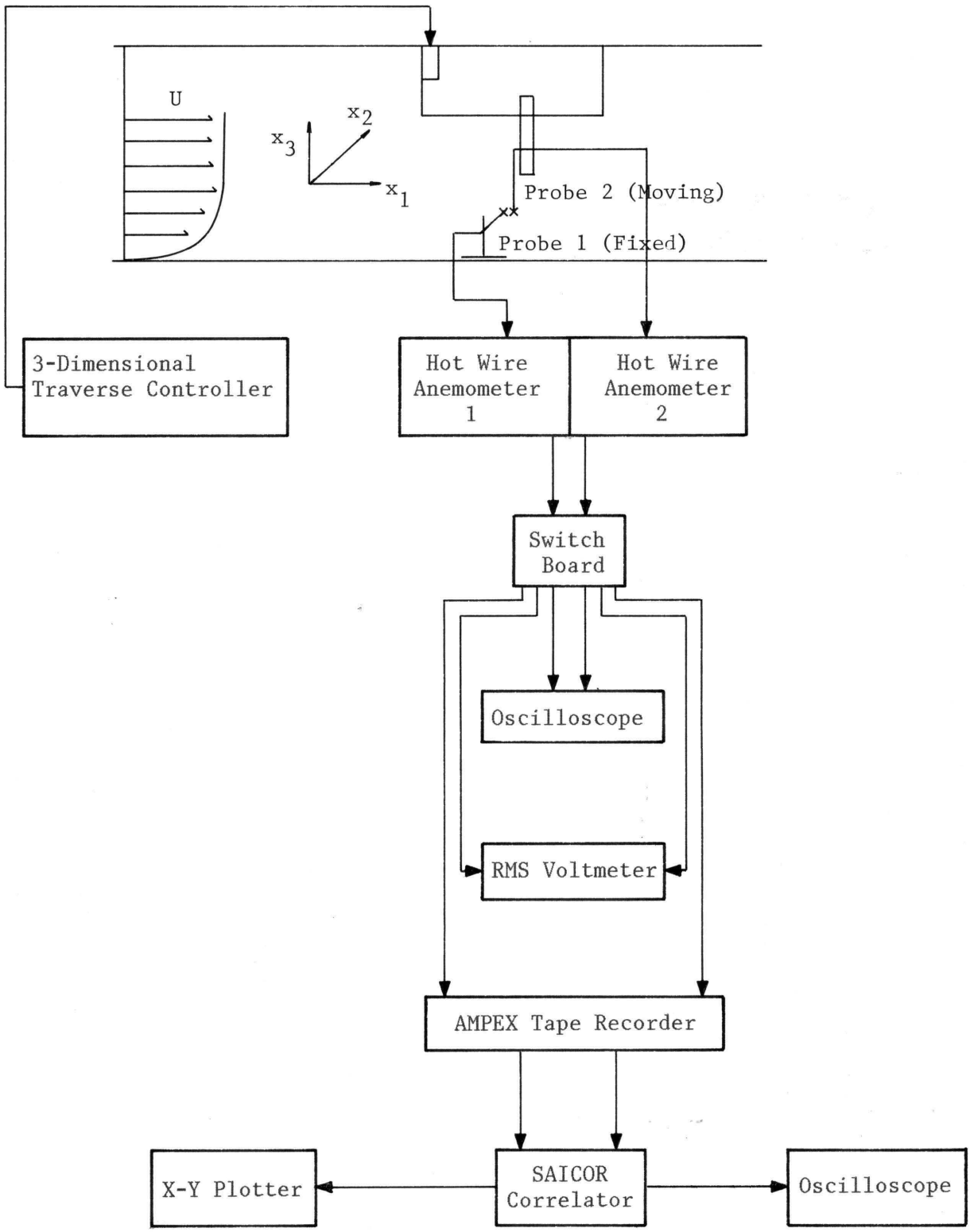

TABLE 5
Comparison of the Lagrangian time scale

$\alpha = 0.2283$	Gaussian	Exponential	Saffman	Philip	Comte-Bellot	Present Study
T_L/T_s	0.764	0.7364	---	0.910	0.6326	0.7102

$\alpha = 0.2283$	Gaussian[1]	Exponential[2]	Saffman[3]	Philip[4]	Comte-Bellot[5]	Present Study[6]
T_L/T_s	0.6048	0.5564	0.75	0.670	0.4484	0.5332

[1] Eulerian Correlation Function is Gaussian
[2] Eulerian Correlation Function is Exponential
[3] Saffman (1963), $\alpha = 0.53$
[4] Philip (1967)
[5] Comte-Bellot and Corrsin (1971), Tabulated for Grid Turbulence
[6] Eulerian Correlation Function is Measured in a Simulated Atmospheric Boundary Layer

TABLE 6

Dispersion data in the anisotropic homogeneous shear flow, $x_{1s} = 0$, $x_{2s} = 0$, $x_{3s} = 10$ cm, $x_1 = 100$ cm, $U_\infty = 200$ cm/sec

U(FREE STREAM) : 200.0 CM/SEC URMS : 15.5 CM/SEC U(LOCAL VEL.) : 154.9 CM/SEC
RELEASE HEIGHT : 10.0 CM VRMS : 7.0 CM/SEC VEL. GRADIENT : 2.593 1/SEC
DOWNWIND DIST. : 100.0 CM WRMS : 7.0 CM/SEC SOURCE STRENGTH : 10 % ETHANE

(A) DIFFUSION MEASUREMENTS IN THE WIND TUNNEL (PPM)

Z/Y (CM)	0.0	5.0	10.0	15.0	20.0	25.0	30.0	35.0
20.0	.5979E+02	.3940E+02	.9141E+01	.1083E+01	.1425E+00	0.	0.	0.
15.0	.8675E+02	.6070E+02	.1399E+02	.1921E+01	.3718E+00	.1245E+00	0.	.6224E-01
10.0	.5748E+02	.4181E+02	.1168E+02	.1310E-01	.1327E+00	.3489E+00	.1474E+00	0.
5.0	.2009E+02	.1378E+02	.5385E+01	.5454E+00	0.	0.	.1965E-01	0.
0.0	.3665E+01	.2257E+01	.8320E+00	.7698E-01	0.	0.	0.	0.

(B) EQUATION 3-16 WITH CONSTANT DIFFUSIVITIES (PPM)

Z/Y (CM)	0.0	5.0	10.0	15.0	20.0	25.0	30.0	35.0
20.0	.3828E-33	.7017E-34	.4324E-36	.8953E-40	.6231E-45	.1457E-51	.1146E-59	.3027E-69
15.0	.5290E-23	.9699E-24	.5976E-26	.1237E-29	.8612E-35	.2014E-41	.1584E-49	.4184E-59
10.0	.2289E-15	.4196E-16	.2585E-18	.5353E-22	.3726E-27	.8715E-34	.6851E-42	.1810E-51
5.0	.3919E-10	.7184E-11	.4426E-13	.9166E-17	.6379E-22	.1492E-28	.1173E-36	.3099E-46
0.0	.3243E-07	.5944E-08	.3663E-10	.7584E-14	.5278E-19	.1235E-25	.9706E-34	.2564E-43

(C) EQUATION 3-18 WITH CONSTANT DIFFUSIVITIES (PPM)

Z/Y (CM)	0.0	5.0	10.0	15.0	20.0	25.0	30.0	35.0
20.0	.3337E+00	.6118E-01	.3770E-03	.7806E-07	.5433E-12	.1271E-18	.9990E-27	.2639E-36
15.0	.8658E+02	.1587E+02	.9780E-01	.2025E-04	.1409E-09	.3297E-16	.2592E-24	.6847E-34
10.0	.5227E+03	.9582E+02	.5904E+00	.1223E-03	.8508E-09	.1990E-15	.1564E-23	.4134E-33
5.0	.1053E+03	.1931E+02	.1190E+00	.2464E-04	.1715E-09	.4011E-16	.3153E-24	.8331E-34
0.0	.3440E+01	.6307E+00	.3886E-02	.8047E-06	.5600E-11	.1310E-17	.1030E-25	.2721E-35

(D) EQUATION 3-18 WITH VARYING DIFFUSIVITIES (PPM)

Z/Y (CM)	0.0	5.0	10.0	15.0	20.0	25.0	30.0	35.0
20.0	.2845E+01	.5215E+00	.3213E-02	.6654E-06	.4631E-11	.1083E-17	.8515E-26	.2250E-35
15.0	.1104E+03	.2024E+02	.1247E+00	.2583E-04	.1798E-09	.4205E-16	.3305E-24	.8733E-34
10.0	.5234E+03	.9596E+02	.5913E+00	.1224E-03	.8521E-09	.1993E-15	.1567E-23	.4140E-33
5.0	.6875E+02	.1260E+02	.7766E-01	.1608E-04	.1119E-09	.2618E-16	.2058E-24	.5437E-34
0.0	.5077E-04	.9308E-05	.5735E-07	.1188E-10	.8265E-16	.1933E-22	.1520E-30	.4015E-40

TABLE 7

Dispersion data in the anisotropic homogeneous shear flow, $x_{1s} = 0$, $x_{2s} = 0$, $x_{3s} = 10$ cm, $x_1 = 200$ cm, $U_\infty = 200$ cm/sec

U(FREE STREAM) : 200.0 CM/SEC		URMS : 15.5 CM/SEC		U(LOCAL VEL.) : 154.9 CM/SEC				
RELEASE HEIGHT : 10.0 CM		VRMS : 7.0 CM/SEC		VEL. GRADIENT : 2.593 1/SEC				
DOWNWIND DIST. : 200.0 CM		WRMS : 7.0 CM/SEC		SOURCE STRENGTH : 10 % ETHANE				

(A) DIFFUSION MEASUREMENTS IN THE WIND TUNNEL (PPM)

20.0	.3508E+02	.2983E+02	.1807E+02	.7323E+01	.2326E+01	.3949E+00	.3095E+00	.1322E+00
15.0	.4190E+02	.3647E+02	.2216E+02	.9586E+01	.3034E+01	.7721E+00	0.	.6931E-01
10.0	.3774E+02	.3052E+02	.2069E+02	.3153E+01	.2787E+01	.7463E+00	.2079E+00	0.
5.0	.2512E+02	.2110E+02	.1396E+02	.5645E+01	.2150E+01	.6834E+00	.7576E-01	.2917E+00
0.0	.1367E+02	.1056E+02	.6728E+01	.2697E+01	.1312E+01	.5335E+00	.9832E-01	.2901E+00
Z/Y (CM)	0.0	5.0	10.0	15.0	20.0	25.0	30.0	35.0

(B) EQUATION 3-16 WITH CONSTANT DIFFUSIVITIES (PPM)

20.0	.3251E-02	.1392E-02	.1093E-03	.1572E-05	.4148E-08	.2006E-11	.1779E-15	.2891E-20
15.0	.2042E+01	.8742E+00	.6862E-01	.9874E-03	.2605E-05	.1260E-08	.1117E-12	.1816E-17
10.0	.5498E+02	.2354E+02	.1848E+01	.2659E-01	.7015E-04	.3393E-07	.3008E-11	.4889E-16
5.0	.8265E+02	.3539E+02	.2778E+01	.3997E-01	.1055E-03	.5100E-07	.4522E-11	.7350E-16
0.0	.1194E+02	.5113E+01	.4013E+00	.5775E-02	.1523E-04	.7368E-08	.6533E-12	.1062E-16
Z/Y (CM)	0.0	5.0	10.0	15.0	20.0	25.0	30.0	35.0

(C) EQUATION 3-18 WITH CONSTANT DIFFUSIVITIES (PPM)

20.0	.6512E+01	.2788E+01	.2188E+00	.3149E-02	.8308E-05	.4018E-08	.3563E-12	.5791E-17
15.0	.1056E+03	.4520E+02	.3548E+01	.5105E-01	.1347E-03	.6514E-07	.5775E-11	.9387E-16
10.0	.2618E+03	.1121E+03	.8799E+01	.1266E+00	.3340E-03	.1616E-06	.1432E-10	.2328E-15
5.0	.1202E+03	.5147E+02	.4040E+01	.5814E-01	.1534E-03	.7418E-07	.6577E-11	.1069E-15
0.0	.3126E+02	.1338E+02	.1051E+01	.1512E-01	.3988E-04	.1929E-07	.1710E-11	.2780E-16
Z/Y (CM)	0.0	5.0	10.0	15.0	20.0	25.0	30.0	35.0

(D) EQUATION 3-18 WITH VARYING DIFFUSIVITIES (PPM)

20.0	.1747E+02	.7479E+01	.5871E+00	.8448E-02	.2229E-04	.1078E-07	.9557E-12	.1553E-16
15.0	.1136E+03	.4862E+02	.3817E+01	.5492E-01	.1449E-03	.7007E-07	.6213E-11	.1010E-15
10.0	.2626E+03	.1124E+03	.8824E+01	.1270E+00	.3350E-03	.1620E-06	.1437E-10	.2335E-15
5.0	.1055E+03	.4519E+02	.3547E+01	.5104E-01	.1347E-03	.6512E-07	.5774E-11	.9385E-16
0.0	.1758E+00	.7529E-01	.5910E-02	.8505E-04	.2244E-06	.1085E-09	.9621E-14	.1564E-18
Z/Y (CM)	0.0	5.0	10.0	15.0	20.0	25.0	30.0	35.0

TABLE 8

Dispersion data in the anisotropic homogeneous shear flow, $x_{1s} = 0$, $x_{2s} = 0$, $x_{3s} = 10$ cm, $x_1 = 500$ cm, $U_\infty = 200$ cm/sec

U(FREE STREAM) : 200.0 CM/SEC		URMS : 15.5 CM/SEC		U(LOCAL VEL.) : 154.9 CM/SEC				
RELEASE HEIGHT : 10.0 CM		VRMS : 7.0 CM/SEC		VEL. GRADIENT : 2.593 1/SEC				
DOWNWIND DIST. : 500.0 CM		WRMS : 7.0 CM/SEC		SOURCE STRENGTH : 10 % ETHANE				

(A) DIFFUSION MEASUREMENTS IN THE WIND TUNNEL (PPM)

20.0	.1359E+02	.1280E+02	.1128E+02	.8918E+01	.6449E+01	.4128E+01	.2864E+01	.1568E+01
15.0	.1459E+02	.1387E+02	.1216E+02	.9697E+01	.7134E+01	.4576E+01	0.	.1642E+01
10.0	.1485E+02	0.	.1230E+02	.6246E+01	.7137E+01	.4942E+01	.2895E+01	.5980E+00
5.0	.1437E+02	.1413E+02	.1258E+02	.9736E+01	.7395E+01	.4797E+01	.2805E+01	.1797E+01
0.0	.1509E+02	.1395E+02	.1193E+02	0.	.7036E+01	.4591E+01	.2663E+01	.1642E+01
Z/Y (CM)	0.0	5.0	10.0	15.0	20.0	25.0	30.0	35.0

(B) EQUATION 3-16 WITH CONSTANT DIFFUSIVITIES (PPM)

20.0	.2326E+02	.1656E+02	.5985E+01	.1097E+01	.1021E+00	.4816E-02	.1153E-03	.1400E-05
15.0	.7238E+02	.5155E+02	.1863E+02	.3415E+01	.3176E+00	.1499E-01	.3588E-03	.4357E-05
10.0	.1052E+03	.7491E+02	.2707E+02	.4963E+01	.4616E+00	.2178E-01	.5214E-03	.6332E-05
5.0	.7769E+02	.5533E+02	.1999E+02	.3666E+01	.3409E+00	.1609E-01	.3851E-03	.4677E-05
0.0	.3179E+02	.2265E+02	.8183E+01	.1500E+01	.1395E+00	.6584E-02	.1576E-03	.1914E-05
Z/Y (CM)	0.0	5.0	10.0	15.0	20.0	25.0	30.0	35.0

(C) EQUATION 3-18 WITH CONSTANT DIFFUSIVITIES (PPM)

20.0	.2352E+02	.1676E+02	.6055E+01	.1110E+01	.1032E+00	.4871E-02	.1166E-03	.1416E-05
15.0	.7237E+02	.5155E+02	.1863E+02	.3415E+01	.3176E+00	.1499E-01	.3587E-03	.4357E-05
10.0	.1064E+03	.7582E+02	.2740E+02	.5023E+01	.4672E+00	.2204E-01	.5277E-03	.6409E-05
5.0	.8762E+02	.6241E+02	.2255E+02	.4134E+01	.3845E+00	.1814E-01	.4343E-03	.5275E-05
0.0	.6993E+02	.4981E+02	.1800E+02	.3300E+01	.3069E+00	.1448E-01	.3466E-03	.4210E-05
Z/Y (CM)	0.0	5.0	10.0	15.0	20.0	25.0	30.0	35.0

(D) EQUATION 3-18 WITH VARYING DIFFUSIVITIES (PPM)

20.0	.3163E+02	.2253E+02	.8142E+01	.1493E+01	.1388E+00	.6551E-02	.1568E-03	.1904E-05
15.0	.7046E+02	.5019E+02	.1814E+02	.3325E+01	.3092E+00	.1459E-01	.3493E-03	.4242E-05
10.0	.1061E+03	.7558E+02	.2731E+02	.5007E+01	.4657E+00	.2197E-01	.5260E-03	.6388E-05
5.0	.8386E+02	.5973E+02	.2158E+02	.3957E+01	.3680E+00	.1737E-01	.4157E-03	.5049E-05
0.0	.1381E+02	.9835E+01	.3554E+01	.6516E+00	.6060E-01	.2859E-02	.6845E-04	.8313E-06
Z/Y (CM)	0.0	5.0	10.0	15.0	20.0	25.0	30.0	35.0

TABLE 9

Dispersion data in the isotropic homogeneous shear flow, $x_{1s} = 0$, $x_{2s} = 0$, $x_{3s} = 10$ cm, $x_1 = 100$ cm, $U_\infty = 200$ cm/sec

U(FREE STREAM) : 200.0 CM/SEC	URMS : 15.5 CM/SEC	U(LOCAL VEL.) : 154.9 CM/SEC	
RELEASE HEIGHT : 10.0 CM	VRMS : 15.5 CM/SEC	VEL. GRADIENT : 2.593 1/SEC	
DOWNWIND DIST. : 100.0 CM	WRMS : 15.5 CM/SEC	SOURCE STRENGTH : 10 % ETHANE	

(A) DIFFUSION MEASUREMENTS IN THE WIND TUNNEL (PPM)

20.0	.5979E+02	.3940E+02	.9141E+01	.1083E+01	.1425E+00	0.	0.	0.
15.0	.8675E+02	.6070E+02	.1399E+02	.1921E+01	.3718E+00	.1245E+00	0.	.6224E-01
10.0	.5748E+02	.4181E+02	.1168E+02	.1310E-01	.1327E+00	.3489E+00	.1474E+00	0.
5.0	.2009E+02	.1378E+02	.5385E+01	.5454E+00	0.	0.	.1965E-01	0.
0.0	.3665E+01	.2257E+01	.8320E+00	.7698E-01	0.	0.	0.	0.
Z/Y (CM)	0.0	5.0	10.0	15.0	20.0	25.0	30.0	35.0

(B) EQUATION 3-16 WITH CONSTANT DIFFUSIVITIES (PPM)

20.0	.2316E+02	.1645E+02	.5894E+01	.1065E+01	.9709E-01	.4465E-02	.1036E-03	.1212E-05
15.0	.7277E+02	.5168E+02	.1852E+02	.3346E+01	.3050E+00	.1403E-01	.3254E-03	.3807E-05
10.0	.1061E+03	.7533E+02	.2699E+02	.4877E+01	.4446E+00	.2044E-01	.4742E-03	.5549E-05
5.0	.7813E+02	.5549E+02	.1988E+02	.3593E+01	.3275E+00	.1506E-01	.3493E-03	.4087E-05
0.0	.3173E+02	.2253E+02	.8073E+01	.1459E+01	.1330E+00	.6116E-02	.1419E-03	.1660E-05
Z/Y (CM)	0.0	5.0	10.0	15.0	20.0	25.0	30.0	35.0

(C) EQUATION 3-18 WITH CONSTANT DIFFUSIVITIES (PPM)

20.0	.2343E+02	.1664E+02	.5962E+01	.1077E+01	.9821E-01	.4516E-02	.1048E-03	.1226E-05
15.0	.7275E+02	.5167E+02	.1851E+02	.3345E+01	.3050E+00	.1402E-01	.3253E-03	.3806E-05
10.0	.1073E+03	.7621E+02	.2730E+02	.4934E+01	.4498E+00	.2068E-01	.4798E-03	.5614E-05
5.0	.8795E+02	.6247E+02	.2238E+02	.4044E+01	.3687E+00	.1695E-01	.3933E-03	.4601E-05
0.0	.6985E+02	.4961E+02	.1777E+02	.3212E+01	.2928E+00	.1346E-01	.3123E-03	.3654E-05
Z/Y (CM)	0.0	5.0	10.0	15.0	20.0	25.0	30.0	35.0

(D) EQUATION 3-18 WITH VARYING DIFFUSIVITIES (PPM)

20.0	.3163E+02	.2246E+02	.8048E+01	.1454E+01	.1326E+00	.6097E-02	.1414E-03	.1655E-05
15.0	.7088E+02	.5034E+02	.1803E+02	.3259E+01	.2971E+00	.1366E-01	.3169E-03	.3708E-05
10.0	.1070E+03	.7598E+02	.2722E+02	.4920E+01	.4485E+00	.2062E-01	.4784E-03	.5597E-05
5.0	.8423E+02	.5982E+02	.2143E+02	.3873E+01	.3531E+00	.1624E-01	.3766E-03	.4407E-05
0.0	.1353E+02	.9609E+01	.3442E+01	.6221E+00	.5671E-01	.2608E-02	.6049E-04	.7078E-06
Z/Y (CM)	0.0	5.0	10.0	15.0	20.0	25.0	30.0	35.0

TABLE 10

Dispersion data in the isotropic homogeneous shear flow, $x_{1s} = 0$, $x_{2s} = 0$, $x_{3s} = 10$ cm, $x_1 = 200$ cm, $U_\infty = 200$ cm/sec

U(FREE STREAM) : 200.0 CM/SEC		URMS : 15.5 CM/SEC		U(LOCAL VEL.) : 154.9 CM/SEC				
RELEASE HEIGHT : 10.0 CM		VRMS : 15.5 CM/SEC		VEL. GRADIENT : 2.593 1/SEC				
DOWNWIND DIST. : 200.0 CM		WRMS : 15.5 CM/SEC		SOURCE STRENGTH : 10 % ETHANE				

(A) DIFFUSION MEASUREMENTS IN THE WIND TUNNEL (PPM)

20.0	.3508E+02	.2983E+02	.1807E+02	.7323E+01	.2326E+01	.3949E+00	.3095E+00	.1322E+00
15.0	.4190E+02	.3647E+02	.2216E+02	.9586E+01	.3034E+01	.7721E+00	0.	.6931E-01
10.0	.3774E+02	.3052E+02	.2069E+02	.3153E+01	.2787E+01	.7463E+00	.2079E+00	0.
5.0	.2512E+02	.2110E+02	.1396E+02	.5645E+01	.2150E+01	.6834E+00	.7576E-01	.2917E+00
0.0	.1367E+02	.1056E+02	.6728E+01	.2697E+01	.1312E+01	.5335E+00	.9832E-01	.2901E+00
Z/Y (CM)	0.0	5.0	10.0	15.0	20.0	25.0	30.0	35.0

(B) EQUATION 3-16 WITH CONSTANT DIFFUSIVITIES (PPM)

20.0	.2433E+02	.2051E+02	.1228E+02	.5218E+01	.1576E+01	.3379E+00	.5146E-01	.5566E-02
15.0	.4355E+02	.3670E+02	.2197E+02	.9338E+01	.2819E+01	.6046E+00	.9208E-01	.9960E-02
10.0	.5312E+02	.4477E+02	.2679E+02	.1139E+02	.3439E+01	.7375E+00	.1123E+00	.1215E-01
5.0	.4611E+02	.3886E+02	.2326E+02	.9887E+01	.2985E+01	.6401E+00	.9750E-01	.1055E-01
0.0	.2975E+02	.2507E+02	.1501E+02	.6379E+01	.1926E+01	.4130E+00	.6291E-01	.6805E-02
Z/Y (CM)	0.0	5.0	10.0	15.0	20.0	25.0	30.0	35.0

(C) EQUATION 3-18 WITH CONSTANT DIFFUSIVITIES (PPM)

20.0	.2483E+02	.2092E+02	.1252E+02	.5324E+01	.1608E+01	.3447E+00	.5250E-01	.5679E-02
15.0	.4497E+02	.3790E+02	.2268E+02	.9643E+01	.2911E+01	.6243E+00	.9509E-01	.1029E-01
10.0	.5866E+02	.4944E+02	.2959E+02	.1258E+02	.3798E+01	.8144E+00	.1240E+00	.1342E-01
5.0	.6179E+02	.5207E+02	.3117E+02	.1325E+02	.4000E+01	.8578E+00	.1307E+00	.1413E-01
0.0	.6139E+02	.5173E+02	.3097E+02	.1316E+02	.3975E+01	.8523E+00	.1298E+00	.1404E-01
Z/Y (CM)	0.0	5.0	10.0	15.0	20.0	25.0	30.0	35.0

(D) EQUATION 3-18 WITH VARYING DIFFUSIVITIES (PPM)

20.0	.2653E+02	.2236E+02	.1338E+02	.5689E+01	.1718E+01	.3683E+00	.5609E-01	.6068E-02
15.0	.4157E+02	.3503E+02	.2097E+02	.8913E+01	.2691E+01	.5771E+00	.8789E-01	.9507E-02
10.0	.5456E+02	.4598E+02	.2752E+02	.1170E+02	.3533E+01	.7575E+00	.1154E+00	.1248E-01
5.0	.5464E+02	.4605E+02	.2756E+02	.1172E+02	.3538E+01	.7586E+00	.1155E+00	.1250E-01
0.0	.3503E+02	.2952E+02	.1767E+02	.7512E+01	.2268E+01	.4863E+00	.7407E-01	.8012E-02
Z/Y (CM)	0.0	5.0	10.0	15.0	20.0	25.0	30.0	35.0

TABLE 11

Dispersion data in the isotropic homogeneous shear flow, $x_{1s} = 0$, $x_{2s} = 0$, $x_{3s} = 10$ cm, $x_1 = 500$ cm, $U_\infty = 200$ cm/sec

U(FREE STREAM)	: 200.0 CM/SEC	URMS	: 15.5 CM/SEC	U(LOCAL VEL.)	: 154.9 CM/SEC			
RELEASE HEIGHT	: 10.0 CM	VRMS	: 15.5 CM/SEC	VEL. GRADIENT	: 2.593 1/SEC			
DOWNWIND DIST.	: 500.0 CM	WRMS	: 15.5 CM/SEC	SOURCE STRENGTH	: 10 % ETHANE			

(A) DIFFUSION MEASUREMENTS IN THE WIND TUNNEL (PPM)

Z/Y (CM)	0.0	5.0	10.0	15.0	20.0	25.0	30.0	35.0
20.0	.1359E+02	.1280E+02	.1128E+02	.8918E+01	.6449E+01	.4128E+01	.2864E+01	.1568E+01
15.0	.1459E+02	.1387E+02	.1216E+02	.9697E+01	.7134E+01	.4576E+01	0.	.1642E+01
10.0	.1485E+02	0.	.1230E+02	.6246E+01	.7137E+01	.4942E+01	.2895E+01	.5980E+00
5.0	.1437E+02	.1413E+02	.1258E+02	.9736E+01	.7395E+01	.4797E+01	.2805E+01	.1797E+01
0.0	.1509E+02	.1395E+02	.1193E+02	0.	.7036E+01	.4591E+01	.2663E+01	.1642E+01

(B) EQUATION 3-16 WITH CONSTANT DIFFUSIVITIES (PPM)

Z/Y (CM)	0.0	5.0	10.0	15.0	20.0	25.0	30.0	35.0
20.0	.1525E+02	.1424E+02	.1160E+02	.8236E+01	.5101E+01	.2756E+01	.1298E+01	.5333E+00
15.0	.1947E+02	.1819E+02	.1481E+02	.1052E+02	.6515E+01	.3519E+01	.1658E+01	.6811E+00
10.0	.2136E+02	.1995E+02	.1624E+02	.1154E+02	.7146E+01	.3860E+01	.1818E+01	.7470E+00
5.0	.2047E+02	.1912E+02	.1557E+02	.1106E+02	.6849E+01	.3700E+01	.1743E+01	.7160E+00
0.0	.1746E+02	.1630E+02	.1328E+02	.9428E+01	.5840E+01	.3154E+01	.1486E+01	.6104E+00

(C) EQUATION 3-18 WITH CONSTANT DIFFUSIVITIES (PPM)

Z/Y (CM)	0.0	5.0	10.0	15.0	20.0	25.0	30.0	35.0
20.0	.1761E+02	.1644E+02	.1339E+02	.9511E+01	.5891E+01	.3182E+01	.1499E+01	.6158E+00
15.0	.2412E+02	.2253E+02	.1835E+02	.1303E+02	.8071E+01	.4360E+01	.2054E+01	.8437E+00
10.0	.2950E+02	.2755E+02	.2243E+02	.1593E+02	.9869E+01	.5331E+01	.2511E+01	.1032E+01
5.0	.3280E+02	.3063E+02	.2495E+02	.1772E+02	.1097E+02	.5928E+01	.2792E+01	.1147E+01
0.0	.3379E+02	.3156E+02	.2570E+02	.1825E+02	.1131E+02	.6107E+01	.2877E+01	.1182E+01

(D) EQUATION 3-18 WITH VARYING DIFFUSIVITIES (PPM)

Z/Y (CM)	0.0	5.0	10.0	15.0	20.0	25.0	30.0	35.0
20.0	.1507E+02	.1407E+02	.1146E+02	.8139E+01	.5041E+01	.2723E+01	.1283E+01	.5270E+00
15.0	.1924E+02	.1796E+02	.1463E+02	.1039E+02	.6436E+01	.3476E+01	.1638E+01	.6728E+00
10.0	.2353E+02	.2197E+02	.1790E+02	.1271E+02	.7873E+01	.4253E+01	.2003E+01	.8229E+00
5.0	.2734E+02	.2553E+02	.2079E+02	.1477E+02	.9147E+01	.4941E+01	.2328E+01	.9562E+00
0.0	.2979E+02	.2782E+02	.2266E+02	.1609E+02	.9967E+01	.5384E+01	.2536E+01	.1042E+01

TABLE 12

Dispersion data in the anisotropic homogeneous shear flow, $x_{1s} = 0$, $x_{2s} = 0$, $x_{3s} = 20$ cm, $x_1 = 100$ cm, $U_\infty = 200$ cm/sec

U(FREE STREAM) : 200.0 CM/SEC URMS : 12.3 CM/SEC U(LOCAL VEL.) : 178.5 CM/SEC
RELEASE HEIGHT : 20.0 CM VRMS : 7.0 CM/SEC VEL. GRADIENT : 1.740 1/SEC
DOWNWIND DIST. : 100.0 CM WRMS : 7.0 CM/SEC SOURCE STRENGTH : 10 % ETHANE

(A) DIFFUSION MEASUREMENTS IN THE WIND TUNNEL (PPM)

40.0	.1016E+01	.7643E+00	.4063E+00	.3886E+00	.3099E+00	0.	0.	0.
30.0	.6011E+02	.3048E+02	.4753E+01	.6600E+00	.3886E+00	.2633E+00	0.	0.
20.0	.8271E+02	.4357E+02	.8188E+01	.1686E+00	.3083E+00	.3051E+00	.2489E+00	0.
10.0	.5294E+01	.3749E+01	.1195E+01	.4368E+00	.4528E+00	.3757E+00	0.	0.
0.0	.3115E+00	.3597E+00	.3468E+00	.2537E+00	.3902E+00	0.	0.	0.
Z/Y (CM)	0.0	5.0	10.0	15.0	20.0	25.0	30.0	35.0

(B) EQUATION 3-16 WITH CONSTANT DIFFUSIVITIES (PPM)

40.0	.1097-103	.4119-104	.2181-105	.1628-107	.1713-110	.2543-114	.5321-119	.1570-124
30.0	.1651E-78	.6198E-79	.3282E-80	.2450E-82	.2578E-85	.3827E-89	.8007E-94	.2363E-99
20.0	.8175E-59	.3070E-59	.1625E-60	.1213E-62	.1277E-65	.1895E-69	.3966E-74	.1170E-79
10.0	.2916E-44	.1095E-44	.5796E-46	.4327E-48	.4555E-51	.6759E-55	.1414E-59	.4173E-65
0.0	.1514E-34	.5685E-35	.3010E-36	.2247E-38	.2365E-41	.3510E-45	.7345E-50	.2167E-55
Z/Y (CM)	0.0	5.0	10.0	15.0	20.0	25.0	30.0	35.0

(C) EQUATION 3-18 WITH CONSTANT DIFFUSIVITIES (PPM)

40.0	.1803E-04	.6772E-05	.3585E-06	.2677E-08	.2817E-11	.4181E-15	.8749E-20	.2581E-25
30.0	.4758E+01	.1787E+01	.9460E-01	.7062E-03	.7433E-06	.1103E-09	.2308E-14	.6811E-20
20.0	.2652E+03	.9956E+02	.5271E+01	.3935E-01	.4142E-04	.6147E-08	.1286E-12	.3795E-18
10.0	.6952E+01	.2610E+01	.1382E+00	.1032E-02	.1086E-05	.1612E-09	.3372E-14	.9950E-20
0.0	.1202E-02	.4515E-03	.2390E-04	.1784E-06	.1878E-09	.2787E-13	.5833E-18	.1721E-23
Z/Y (CM)	0.0	5.0	10.0	15.0	20.0	25.0	30.0	35.0

(D) EQUATION 3-18 WITH VARYING DIFFUSIVITIES (PPM)

40.0	.1387E-05	.5209E-06	.2758E-07	.2059E-09	.2167E-12	.3216E-16	.6729E-21	.1985E-26
30.0	.6493E+00	.2438E+00	.1291E-01	.9636E-04	.1014E-06	.1505E-10	.3150E-15	.9294E-21
20.0	.2170E+03	.8149E+02	.4315E+01	.3221E-01	.3390E-04	.5031E-08	.1053E-12	.3106E-18
10.0	.2141E+01	.8041E+00	.4257E-01	.3178E-03	.3345E-06	.4965E-10	.1039E-14	.3065E-20
0.0	.1346E-14	.5055E-15	.2676E-16	.1998E-18	.2103E-21	.3121E-25	.6531E-30	.1927E-35
Z/Y (CM)	0.0	5.0	10.0	15.0	20.0	25.0	30.0	35.0

TABLE 13

Dispersion data in the anisotropic homogeneous shear flow, $x_{1s} = 0$, $x_{2s} = 0$, $x_{3s} = 20$ cm, $x_1 = 200$ cm, $U_\infty = 200$ cm/sec

U(FREE STREAM) : 200.0 CM/SEC		URMS : 12.3 CM/SEC		U(LOCAL VEL.) : 178.5 CM/SEC				
RELEASE HEIGHT : 20.0 CM		VRMS : 7.0 CM/SEC		VEL. GRADIENT : 1.740 1/SEC				
DOWNWIND DIST. : 200.0 CM		WRMS : 7.0 CM/SEC		SOURCE STRENGTH : 10 % ETHANE				

(A) DIFFUSION MEASUREMENTS IN THE WIND TUNNEL (PPM)

40.0	.3264E+01	.2874E+01	.1257E+01	.5303E+00	.1886E+00	0.	.2192E+00	.4836E-01
30.0	.3269E+02	.2523E+02	.1267E+02	.4094E+01	.1094E+01	.1950E+00	0.	0.
20.0	.3991E+02	.3143E+02	.1878E+02	.3320E+00	.1596E+01	.3304E+00	.4191E-01	0.
10.0	.1048E+02	.1019E+02	.6254E+01	.2274E+01	.9397E+00	.3740E+00	0.	.2531E+00
0.0	.7818E+00	.7640E+00	.5400E+00	.1209E+00	.4400E+00	.3014E+00	.2418E-01	0.
Z/Y (CM)	0.0	5.0	10.0	15.0	20.0	25.0	30.0	35.0

(B) EQUATION 3-16 WITH CONSTANT DIFFUSIVITIES (PPM)

40.0	.9879E-26	.6054E-26	.1393E-26	.1204E-27	.3905E-29	.4757E-31	.2176E-33	.3738E-36
30.0	.7771E-16	.4762E-16	.1096E-16	.9467E-18	.3071E-19	.3742E-21	.1712E-23	.2940E-26
20.0	.6372E-09	.3904E-09	.8984E-10	.7762E-11	.2518E-12	.3068E-14	.1403E-16	.2411E-19
10.0	.7321E-05	.4486E-05	.1032E-05	.8919E-07	.2894E-08	.3525E-10	.1612E-12	.2770E-15
0.0	.1515E-03	.9284E-04	.2136E-04	.1846E-05	.5988E-07	.7294E-09	.3337E-11	.5732E-14
Z/Y (CM)	0.0	5.0	10.0	15.0	20.0	25.0	30.0	35.0

(C) EQUATION 3-18 WITH CONSTANT DIFFUSIVITIES (PPM)

40.0	.3409E-01	.2089E-01	.4806E-02	.4153E-03	.1347E-04	.1641E-06	.7508E-09	.1290E-11
30.0	.1762E+02	.1080E+02	.2484E+01	.2146E+00	.6963E-02	.8482E-04	.3880E-06	.6665E-09
20.0	.1327E+03	.8130E+02	.1871E+02	.1616E+01	.5244E-01	.6388E-03	.2922E-05	.5019E-08
10.0	.2182E+02	.1337E+02	.3077E+01	.2659E+00	.8625E-02	.1051E-03	.4807E-06	.8257E-09
0.0	.4229E+00	.2591E+00	.5963E-01	.5152E-02	.1671E-03	.2036E-05	.9314E-08	.1600E-10
Z/Y (CM)	0.0	5.0	10.0	15.0	20.0	25.0	30.0	35.0

(D) EQUATION 3-18 WITH VARYING DIFFUSIVITIES (PPM)

40.0	.3873E+00	.2373E+00	.5461E-01	.4718E-02	.1531E-03	.1865E-05	.8530E-08	.1465E-10
30.0	.2344E+02	.1437E+02	.3305E+01	.2856E+00	.9266E-02	.1129E-03	.5163E-06	.8869E-09
20.0	.1329E+03	.8141E+02	.1873E+02	.1618E+01	.5251E-01	.6397E-03	.2926E-05	.5026E-08
10.0	.1322E+02	.8100E+01	.1864E+01	.1610E+00	.5224E-02	.6364E-04	.2911E-06	.5001E-09
0.0	.6920E-06	.4241E-06	.9757E-07	.8430E-08	.2735E-09	.3332E-11	.1524E-13	.2618E-16
Z/Y (CM)	0.0	5.0	10.0	15.0	20.0	25.0	30.0	35.0

TABLE 14

Dispersion data in the anisotropic homogeneous shear flow, $x_{1s} = 0$, $x_{2s} = 0$, $x_{3s} = 20$ cm, $x_1 = 500$ cm, $U_\infty = 200$ cm/sec

U(FREE STREAM) : 200.0 CM/SEC		URMS : 12.3 CM/SEC		U(LOCAL VEL.) : 178.5 CM/SEC				
RELEASE HEIGHT : 20.0 CM		VRMS : 7.0 CM/SEC		VEL. GRADIENT : 1.740 1/SEC				
DOWNWIND DIST. : 500.0 CM		WRMS : 7.0 CM/SEC		SOURCE STRENGTH : 10 % ETHANE				

(A) DIFFUSION MEASUREMENTS IN THE WIND TUNNEL (PPM)

40.0	.7911E+01	.7481E+01	.6487E+01	.4472E+01	.2755E+01	.1471E+01	.1103E+01	.5299E+00
30.0	.1407E+02	.1268E+02	.1035E+02	.7850E+01	.5456E+01	.3290E+01	0.	.9233E+00
20.0	.1458E+02	.1212E+02	.1064E+02	.3303E+01	.5752E+01	.3640E+01	.2181E+01	0.
10.0	.8936E+01	.8949E+01	.7478E+01	.5763E+01	.4164E+01	.2613E+01	.1338E+01	.9618E+00
0.0	.5766E+01	.5537E+01	.4580E+01	.3298E+01	.2553E+01	.1656E+01	.8109E+00	.6294E+00
Z/Y (CM)	0.0	5.0	10.0	15.0	20.0	25.0	30.0	35.0

(B) EQUATION 3-16 WITH CONSTANT DIFFUSIVITIES (PPM)

40.0	.1036E+01	.8521E+00	.4734E+00	.1778E+00	.4511E-01	.7737E-02	.8968E-03	.7026E-04
30.0	.2136E+02	.1756E+02	.9757E+01	.3664E+01	.9297E+00	.1595E+00	.1848E-01	.1448E-02
20.0	.5256E+02	.4321E+02	.2401E+02	.9014E+01	.2288E+01	.3923E+00	.4548E-01	.3563E-02
10.0	.2565E+02	.2108E+02	.1171E+02	.4399E+01	.1116E+01	.1915E+00	.2219E-01	.1738E-02
0.0	.3294E+01	.2708E+01	.1505E+01	.5650E+00	.1434E+00	.2459E-01	.2851E-02	.2233E-03
Z/Y (CM)	0.0	5.0	10.0	15.0	20.0	25.0	30.0	35.0

(C) EQUATION 3-18 WITH CONSTANT DIFFUSIVITIES (PPM)

40.0	.1912E+01	.1572E+01	.8734E+00	.3280E+00	.8323E-01	.1427E-01	.1655E-02	.1296E-03
30.0	.2345E+02	.1928E+02	.1071E+02	.4023E+01	.1021E+01	.1751E+00	.2030E-01	.1590E-02
20.0	.5320E+02	.4374E+02	.2430E+02	.9125E+01	.2316E+01	.3972E+00	.4604E-01	.3606E-02
10.0	.2662E+02	.2188E+02	.1216E+02	.4565E+01	.1158E+01	.1987E+00	.2303E-01	.1804E-02
0.0	.8485E+01	.6975E+01	.3876E+01	.1455E+01	.3693E+00	.6334E-01	.7342E-02	.5752E-03
Z/Y (CM)	0.0	5.0	10.0	15.0	20.0	25.0	30.0	35.0

(D) EQUATION 3-18 WITH VARYING DIFFUSIVITIES (PPM)

40.0	.4567E+01	.3755E+01	.2086E+01	.7833E+00	.1988E+00	.3410E-01	.3952E-02	.3096E-03
30.0	.2481E+02	.2039E+02	.1133E+02	.4255E+01	.1080E+01	.1852E+00	.2147E-01	.1682E-02
20.0	.5337E+02	.4387E+02	.2438E+02	.9153E+01	.2323E+01	.3984E+00	.4618E-01	.3618E-02
10.0	.2401E+02	.1974E+02	.1097E+02	.4118E+01	.1045E+01	.1792E+00	.2078E-01	.1628E-02
0.0	.7394E-01	.6079E-01	.3377E-01	.1268E-01	.3218E-02	.5520E-03	.6398E-04	.5012E-05
Z/Y (CM)	0.0	5.0	10.0	15.0	20.0	25.0	30.0	35.0

TABLE 15

Dispersion data in the isotropic homogeneous shear flow, $x_{1s} = 0$, $x_{2s} = 0$, $x_{3s} = 20$ cm, $x_1 = 100$ cm, $U_\infty = 200$ cm/sec

U(FREE STREAM) : 200.0 CM/SEC		URMS : 12.3 CM/SEC		U(LOCAL VEL.) : 178.5 CM/SEC				
RELEASE HEIGHT : 20.0 CM		VRMS : 12.3 CM/SEC		VEL. GRADIENT : 1.740 1/SEC				
DOWNWIND DIST. : 100.0 CM		WRMS : 12.3 CM/SEC		SOURCE STRENGTH : 10 % ETHANE				

(A) DIFFUSION MEASUREMENTS IN THE WIND TUNNEL (PPM)

40.0	.1016E+01	.7643E+00	.4063E+00	.3886E+00	.3099E+00	0.	0.	0.
30.0	.6011E+02	.3048E+02	.4753E+01	.6600E+00	.3886E+00	.2633E+00	0.	0.
20.0	.8271E+02	.4357E+02	.8188E+01	.1686E+00	.3083E+00	.3051E+00	.2489E+00	0.
10.0	.5294E+01	.3749E+01	.1195E+01	.4368E+00	.4528E+00	.3757E+00	0.	0.
0.0	.3115E+00	.3597E+00	.3468E+00	.2537E+00	.3902E+00	0.	0.	0.
Z/Y (CM)	0.0	5.0	10.0	15.0	20.0	25.0	30.0	35.0

(B) EQUATION 3-16 WITH CONSTANT DIFFUSIVITIES (PPM)

40.0	.4088E-06	.2985E-06	.1162E-06	.2411E-07	.2667E-08	.1572E-09	.4943E-11	.8283E-13
30.0	.1237E-01	.9030E-02	.3515E-02	.7293E-03	.8067E-04	.4757E-05	.1495E-06	.2506E-08
20.0	.3401E+01	.2483E+01	.9666E+00	.2006E+00	.2219E-01	.1308E-02	.4112E-04	.6892E-06
10.0	.1140E+02	.8324E+01	.3240E+01	.6723E+00	.7437E-01	.4385E-02	.1379E-03	.2310E-05
0.0	.8921E+00	.6514E+00	.2535E+00	.5261E-01	.5819E-02	.3431E-03	.1079E-04	.1808E-06
Z/Y (CM)	0.0	5.0	10.0	15.0	20.0	25.0	30.0	35.0

(C) EQUATION 3-18 WITH CONSTANT DIFFUSIVITIES (PPM)

40.0	.4172E+00	.3046E+00	.1186E+00	.2460E-01	.2721E-02	.1605E-03	.5044E-05	.8453E-07
30.0	.2317E+02	.1692E+02	.6584E+01	.1366E+01	.1511E+00	.8911E-02	.2801E-03	.4694E-05
20.0	.8528E+02	.6227E+02	.2424E+02	.5029E+01	.5563E+00	.3280E-01	.1031E-02	.1728E-04
10.0	.2710E+02	.1978E+02	.7700E+01	.1598E+01	.1767E+00	.1042E-01	.3276E-03	.5490E-05
0.0	.2815E+01	.2056E+01	.8001E+00	.1660E+00	.1836E-01	.1083E-02	.3404E-04	.5704E-06
Z/Y (CM)	0.0	5.0	10.0	15.0	20.0	25.0	30.0	35.0

(D) EQUATION 3-18 WITH VARYING DIFFUSIVITIES (PPM)

40.0	.1870E+01	.1365E+01	.5313E+00	.1103E+00	.1220E-01	.7191E-03	.2261E-04	.3788E-06
30.0	.2687E+02	.1962E+02	.7637E+01	.1585E+01	.1753E+00	.1034E-01	.3249E-03	.5445E-05
20.0	.8545E+02	.6239E+02	.2429E+02	.5039E+01	.5574E+00	.3287E-01	.1033E-02	.1731E-04
10.0	.2090E+02	.1526E+02	.5939E+01	.1232E+01	.1363E+00	.8037E-02	.2527E-03	.4234E-05
0.0	.7666E-03	.5597E-03	.2179E-03	.4521E-04	.5001E-05	.2949E-06	.9269E-08	.1553E-09
Z/Y (CM)	0.0	5.0	10.0	15.0	20.0	25.0	30.0	35.0

TABLE 16

Dispersion data in the isotropic homogeneous shear flow, $x_{1s} = 0$, $x_{2s} = 0$, $x_{3s} = 20$ cm, $x_1 = 200$ cm, $U_\infty = 200$ cm/sec

U(FREE STREAM) : 200.0 CM/SEC	URMS : 12.3 CM/SEC	U(LOCAL VEL.) : 178.5 CM/SEC
RELEASE HEIGHT : 20.0 CM	VRMS : 12.3 CM/SEC	VEL. GRADIENT : 1.740 1/SEC
DOWNWIND DIST. : 200.0 CM	WRMS : 12.3 CM/SEC	SOURCE STRENGTH : 10 % ETHANE

(A) DIFFUSION MEASUREMENTS IN THE WIND TUNNEL (PPM)

40.0	.3264E+01	.2874E+01	.1257E+01	.5303E+00	.1886E+00	0.	.2192E+00	.4836E-01
30.0	.3269E+02	.2523E+02	.1267E+02	.4094E+01	.1094E+01	.1950E+00	0.	0.
20.0	.3991E+02	.3143E+02	.1878E+02	.3320E+00	.1596E+01	.3304E+00	.4191E-01	0.
10.0	.1048E+02	.1019E+02	.6254E+01	.2274E+01	.9397E+00	.3740E+00	0.	.2531E+00
0.0	.7818E+00	.7640E+00	.5400E+00	.1209E+00	.4400E+00	.3014E+00	.2418E-01	0.
Z/Y (CM)	0.0	5.0	10.0	15.0	20.0	25.0	30.0	35.0

(B) EQUATION 3-16 WITH CONSTANT DIFFUSIVITIES (PPM)

40.0	.2542E+01	.2172E+01	.1355E+01	.6172E+00	.2053E+00	.4985E-01	.8838E-02	.1144E-02
30.0	.2135E+02	.1825E+02	.1138E+02	.5186E+01	.1725E+01	.4188E+00	.7425E-01	.9612E-02
20.0	.4228E+02	.3613E+02	.2254E+02	.1027E+02	.3415E+01	.8293E+00	.1470E+00	.1903E-01
10.0	.2385E+02	.2038E+02	.1272E+02	.5793E+01	.1927E+01	.4678E+00	.8295E-01	.1074E-01
0.0	.4619E+01	.3947E+01	.2463E+01	.1122E+01	.3731E+00	.9060E-01	.1606E-01	.2079E-02
Z/Y (CM)	0.0	5.0	10.0	15.0	20.0	25.0	30.0	35.0

(C) EQUATION 3-18 WITH CONSTANT DIFFUSIVITIES (PPM)

40.0	.2941E+01	.2513E+01	.1568E+01	.7142E+00	.2375E+00	.5768E-01	.1023E-01	.1324E-02
30.0	.2206E+02	.1885E+02	.1176E+02	.5358E+01	.1782E+01	.4327E+00	.7672E-01	.9932E-02
20.0	.4277E+02	.3654E+02	.2280E+02	.1039E+02	.3454E+01	.8387E+00	.1487E+00	.1925E-01
10.0	.2505E+02	.2141E+02	.1335E+02	.6083E+01	.2023E+01	.4913E+00	.8711E-01	.1128E-01
0.0	.1135E+02	.9702E+01	.6053E+01	.2757E+01	.9170E+00	.2227E+00	.3948E-01	.5111E-02
Z/Y (CM)	0.0	5.0	10.0	15.0	20.0	25.0	30.0	35.0

(D) EQUATION 3-18 WITH VARYING DIFFUSIVITIES (PPM)

40.0	.5726E+01	.4892E+01	.3052E+01	.1390E+01	.4624E+00	.1123E+00	.1991E-01	.2577E-02
30.0	.2265E+02	.1936E+02	.1208E+02	.5501E+01	.1830E+01	.4443E+00	.7877E-01	.1020E-01
20.0	.4292E+02	.3667E+02	.2288E+02	.1042E+02	.3466E+01	.8418E+00	.1492E+00	.1932E-01
10.0	.2356E+02	.2014E+02	.1256E+02	.5722E+01	.1903E+01	.4622E+00	.8194E-01	.1061E-01
0.0	.3028E+00	.2587E+00	.1614E+00	.7353E-01	.2446E-01	.5939E-02	.1053E-02	.1363E-03
Z/Y (CM)	0.0	5.0	10.0	15.0	20.0	25.0	30.0	35.0

TABLE 17

Dispersion data in the isotropic homogeneous shear flow, $x_{1s} = 0$, $x_{2s} = 0$, $x_3 s = 20$ cm, $x_1 = 500$ cm, $U_\infty = 200$ cm/sec

U(FREE STREAM) : 200.0 CM/SEC	URMS : 12.3 CM/SEC	U(LOCAL VEL.) : 178.5 CM/SEC
RELEASE HEIGHT : 20.0 CM	VRMS : 12.3 CM/SEC	VEL. GRADIENT : 1.740 1/SEC
DOWNWIND DIST. : 500.0 CM	WRMS : 12.3 CM/SEC	SOURCE STRENGTH : 10 % ETHANE

(A) DIFFUSION MEASUREMENTS IN THE WIND TUNNEL (PPM)

40.0	.7911E+01	.7481E+01	.6487E+01	.4472E+01	.2755E+01	.1471E+01	.1103E+01	.5299E+00
30.0	.1407E+02	.1268E+02	.1035E+02	.7850E+01	.5456E+01	.3290E+01	0.	.9233E+00
20.0	.1458E+02	.1212E+02	.1064E+02	.3303E+01	.5752E+01	.3640E+01	.2181E+01	0.
10.0	.8936E+01	.8949E+01	.7478E+01	.5763E+01	.4164E+01	.2613E+01	.1338E+01	.9618E+00
0.0	.5766E+01	.5537E+01	.4580E+01	.3298E+01	.2553E+01	.1656E+01	.8109E+00	.6294E+00
Z/Y (CM)	0.0	5.0	10.0	15.0	20.0	25.0	30.0	35.0

(B) EQUATION 3-16 WITH CONSTANT DIFFUSIVITIES (PPM)

40.0	.5370E+01	.5043E+01	.4176E+01	.3049E+01	.1963E+01	.1114E+01	.5578E+00	.2462E+00
30.0	.1271E+02	.1194E+02	.9883E+01	.7216E+01	.4646E+01	.2637E+01	.1320E+01	.5828E+00
20.0	.1694E+02	.1591E+02	.1318E+02	.9620E+01	.6193E+01	.3516E+01	.1760E+01	.7769E+00
10.0	.1369E+02	.1286E+02	.1065E+02	.7773E+01	.5004E+01	.2841E+01	.1422E+01	.6278E+00
0.0	.7227E+01	.6786E+01	.5619E+01	.4103E+01	.2641E+01	.1500E+01	.7507E+00	.3314E+00
Z/Y (CM)	0.0	5.0	10.0	15.0	20.0	25.0	30.0	35.0

(C) EQUATION 3-18 WITH CONSTANT DIFFUSIVITIES (PPM)

40.0	.5780E+01	.5428E+01	.4494E+01	.3281E+01	.2113E+01	.1199E+01	.6004E+00	.2650E+00
30.0	.1313E+02	.1233E+02	.1021E+02	.7453E+01	.4798E+01	.2724E+01	.1364E+01	.6019E+00
20.0	.1786E+02	.1677E+02	.1389E+02	.1014E+02	.6528E+01	.3706E+01	.1855E+01	.8189E+00
10.0	.1694E+02	.1591E+02	.1317E+02	.9618E+01	.6192E+01	.3515E+01	.1760E+01	.7768E+00
0.0	.1559E+02	.1464E+02	.1212E+02	.8853E+01	.5700E+01	.3236E+01	.1620E+01	.7150E+00
Z/Y (CM)	0.0	5.0	10.0	15.0	20.0	25.0	30.0	35.0

(D) EQUATION 3-18 WITH VARYING DIFFUSIVITIES (PPM)

40.0	.6846E+01	.6428E+01	.5323E+01	.3886E+01	.2502E+01	.1420E+01	.7111E+00	.3139E+00
30.0	.1251E+02	.1175E+02	.9729E+01	.7103E+01	.4573E+01	.2596E+01	.1300E+01	.5737E+00
20.0	.1743E+02	.1636E+02	.1355E+02	.9892E+01	.6369E+01	.3616E+01	.1810E+01	.7989E+00
10.0	.1567E+02	.1472E+02	.1219E+02	.8898E+01	.5729E+01	.3252E+01	.1628E+01	.7186E+00
0.0	.5630E+01	.5287E+01	.4377E+01	.3196E+01	.2058E+01	.1168E+01	.5848E+00	.2581E+00
Z/Y (CM)	0.0	5.0	10.0	15.0	20.0	25.0	30.0	35.0

FIGURES

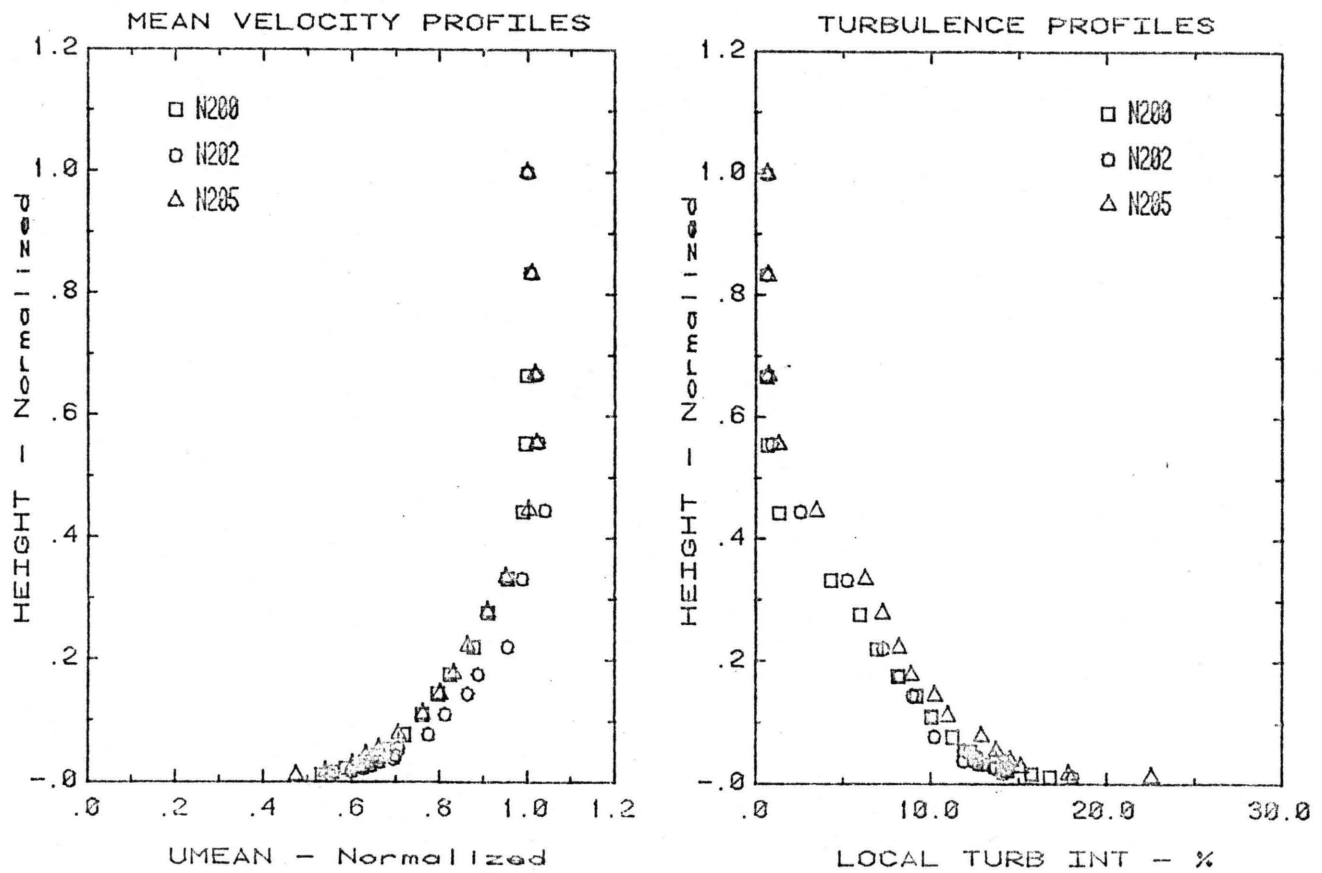

Figure 1. Mean velocity profiles and turbulent intensity profiles, U_∞ = 200 cm/sec

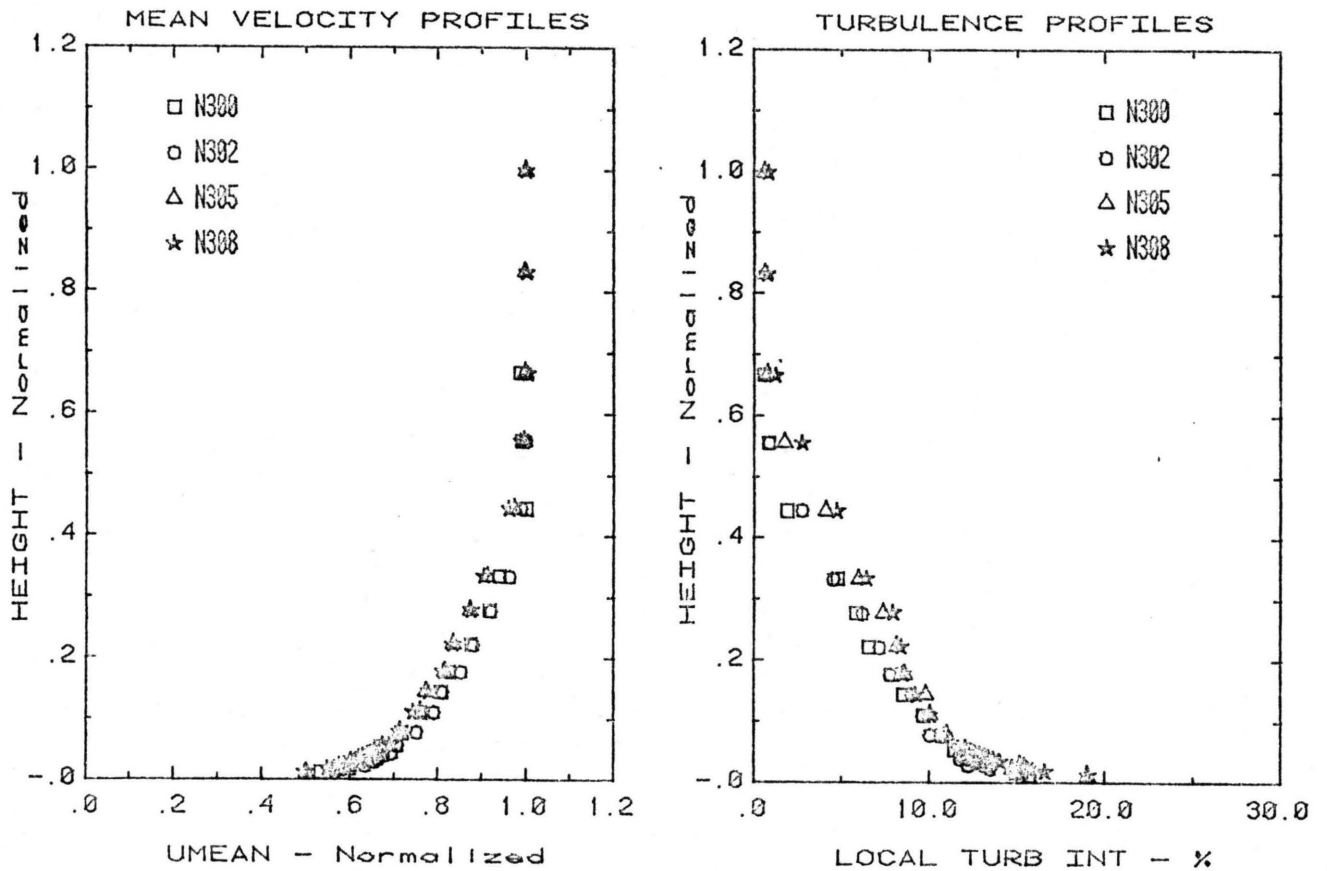

Figure 2. Mean velocity profiles and turbulent intensity profiles, U_∞ = 300 cm/sec

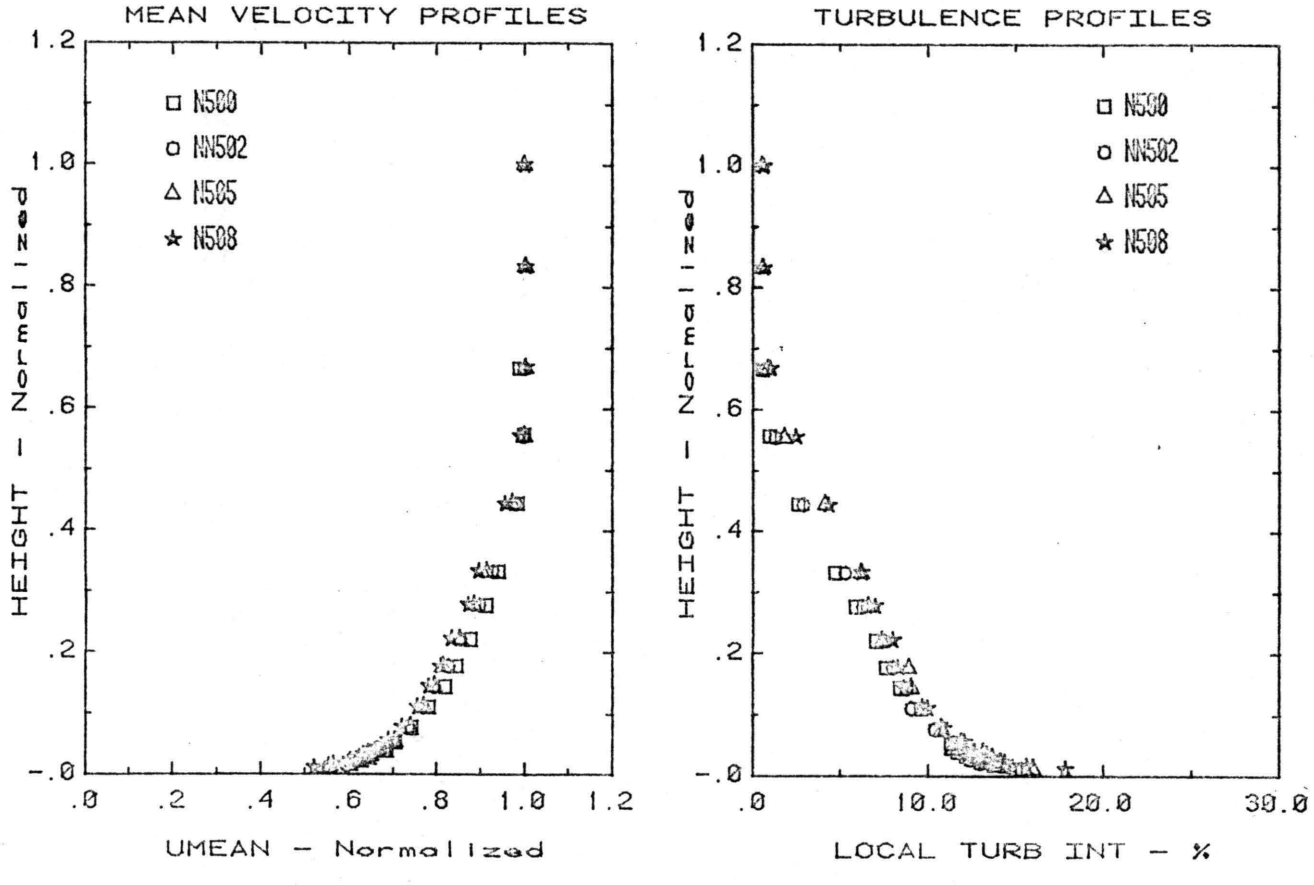

Figure 3. Mean velocity profiles and turbulent intensity profiles, U_{∞} = 500 cm/sec

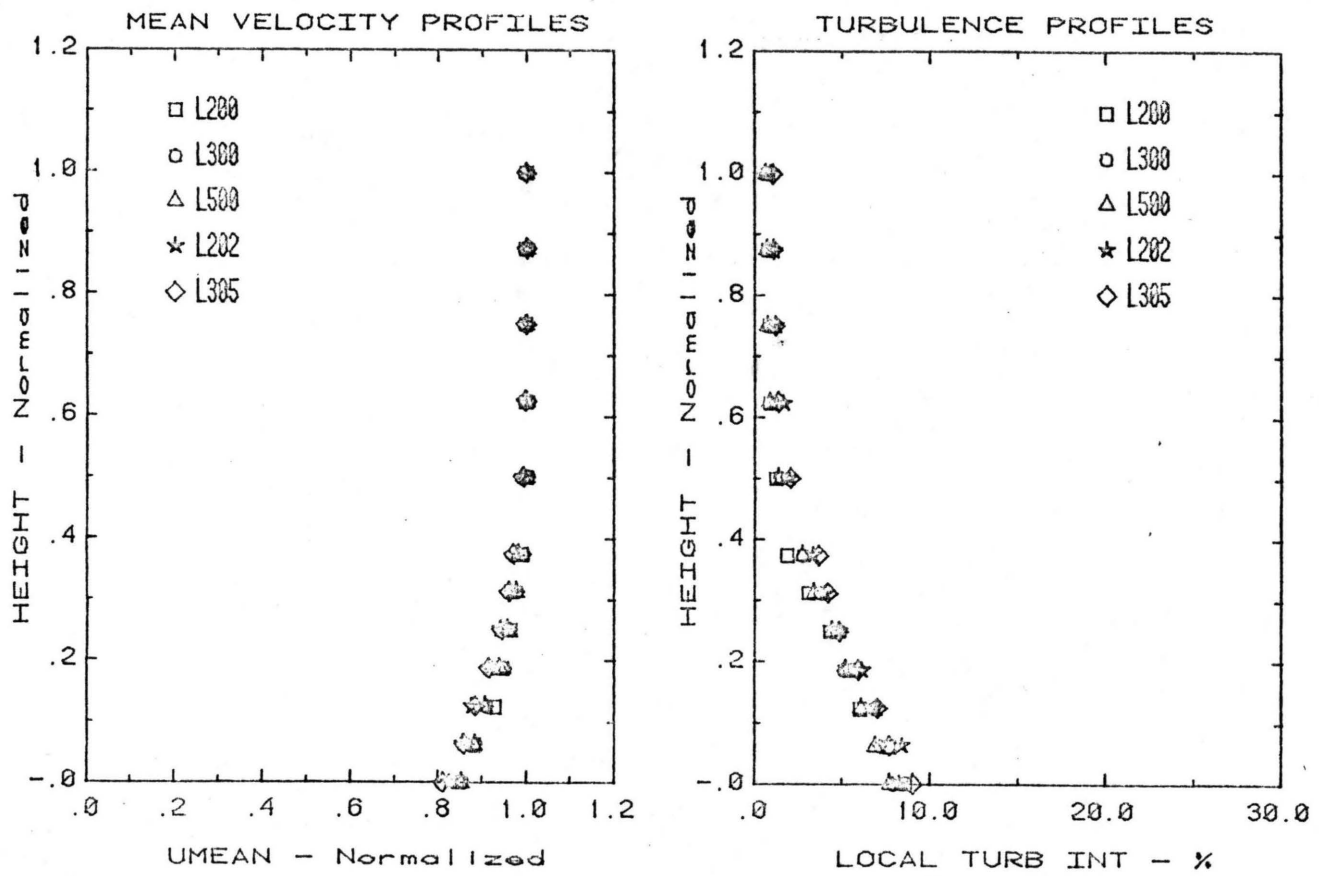

Figure 4. Lateral distribution of mean velocity profiles at 80 cm height

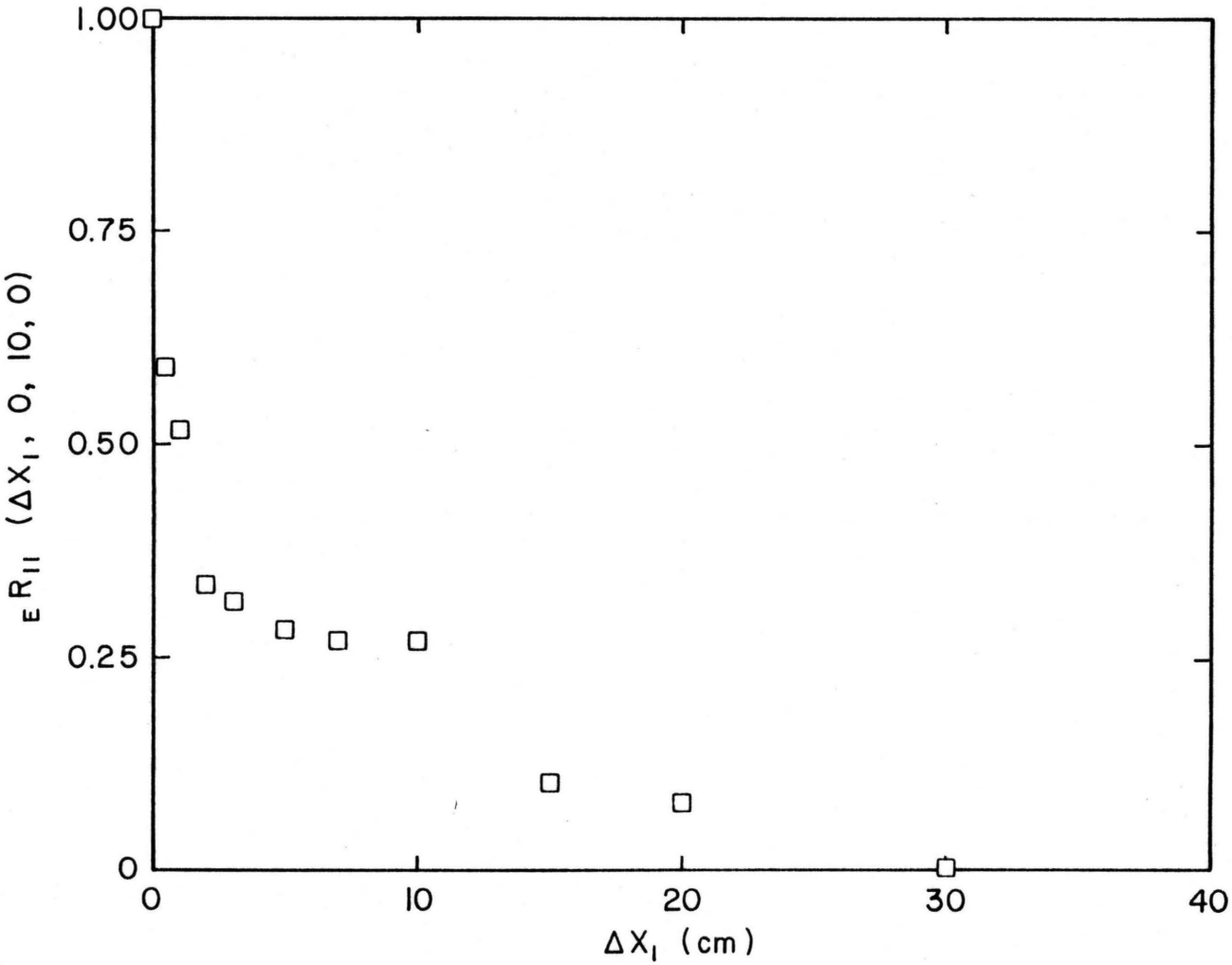

Figure 5. Longitudinal space correlation at 10 cm height, U_∞ = 200 cm/sec

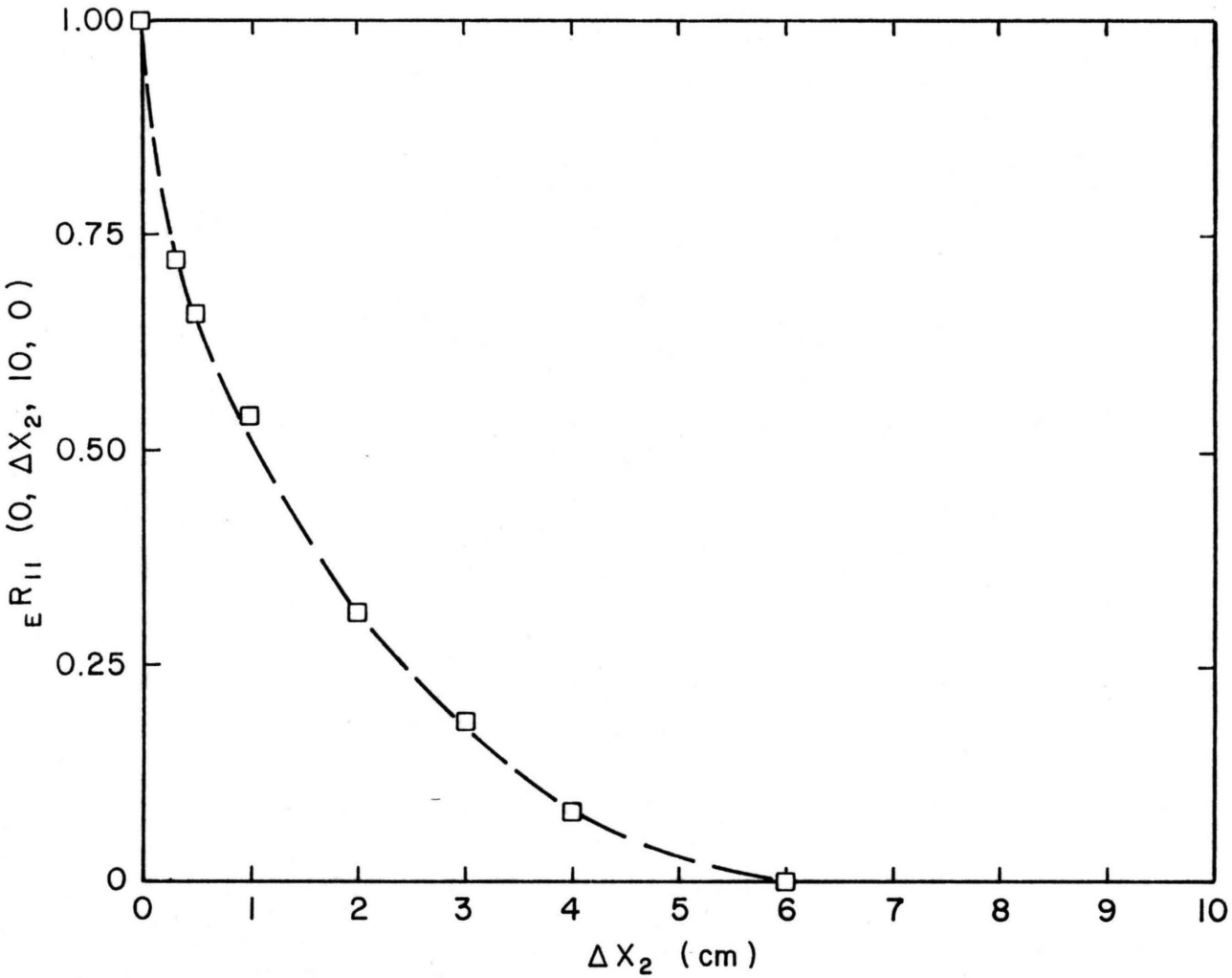

Figure 6. Transverse space correlation at 10 cm height, U_∞ = 200 cm/sec

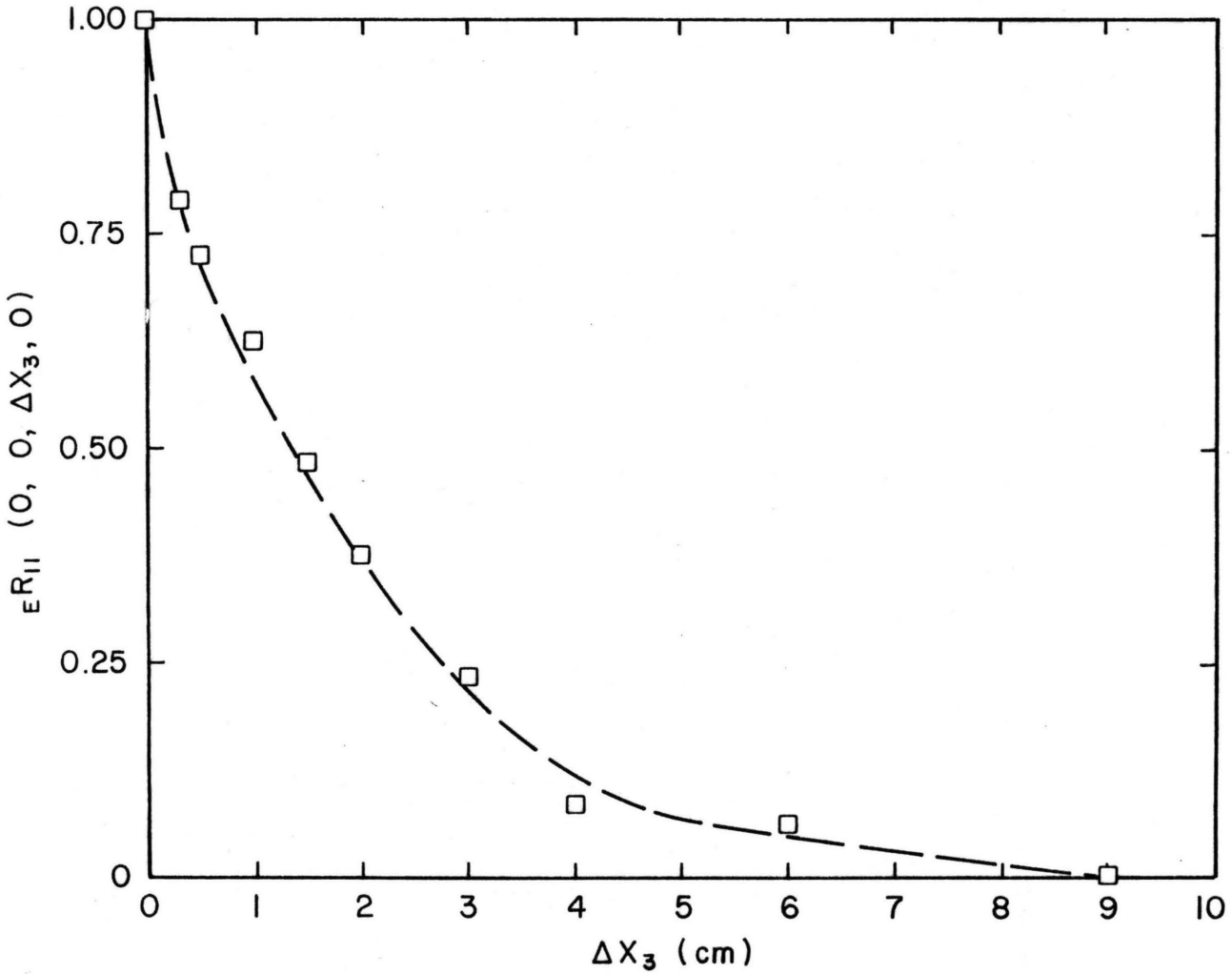

Figure 7. Vertical space correlation at 10 cm height, U_∞ = 200 cm/sec

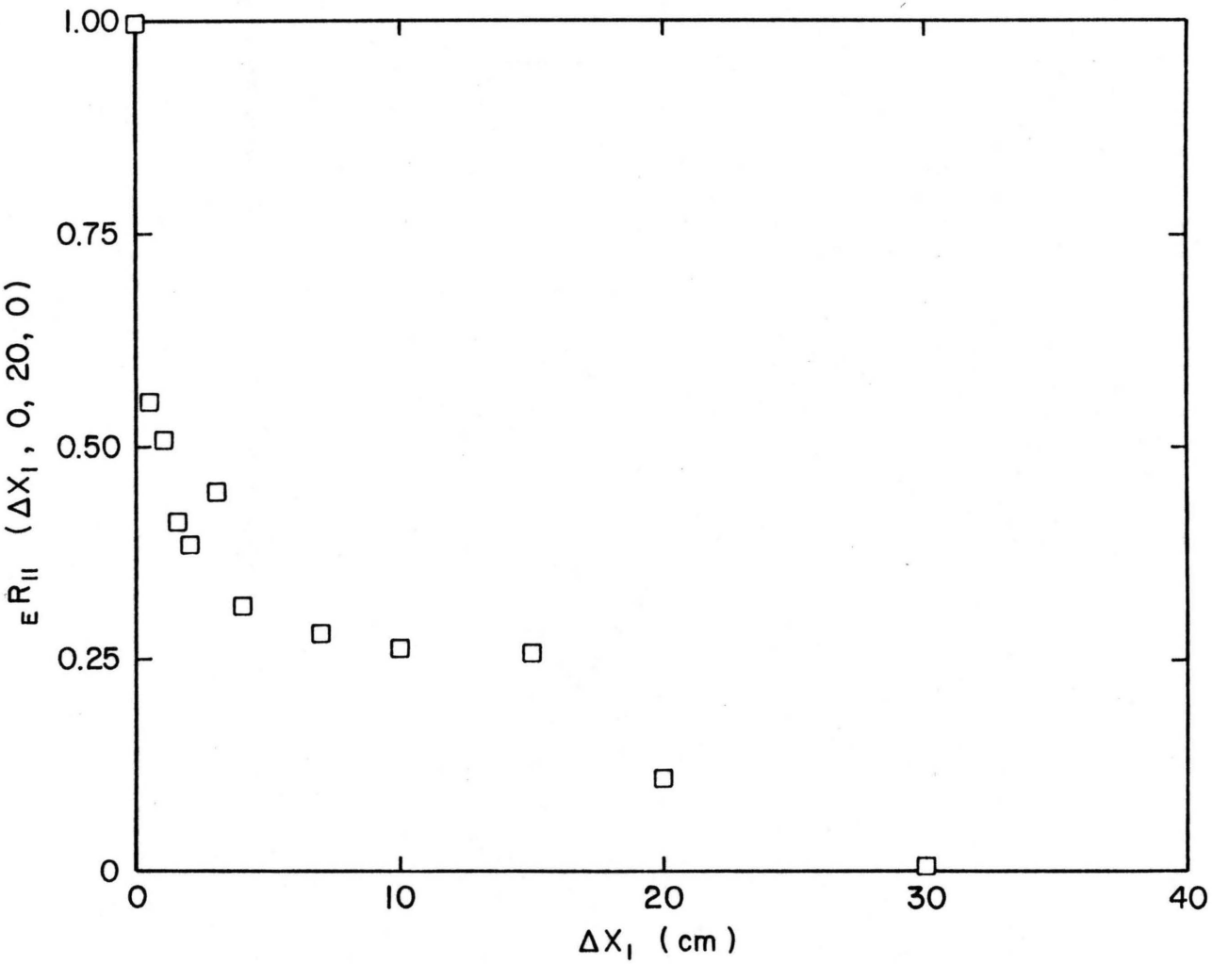

Figure 8. Longitudinal space correlation at 20 cm height, U_∞ = 200 cm/sec

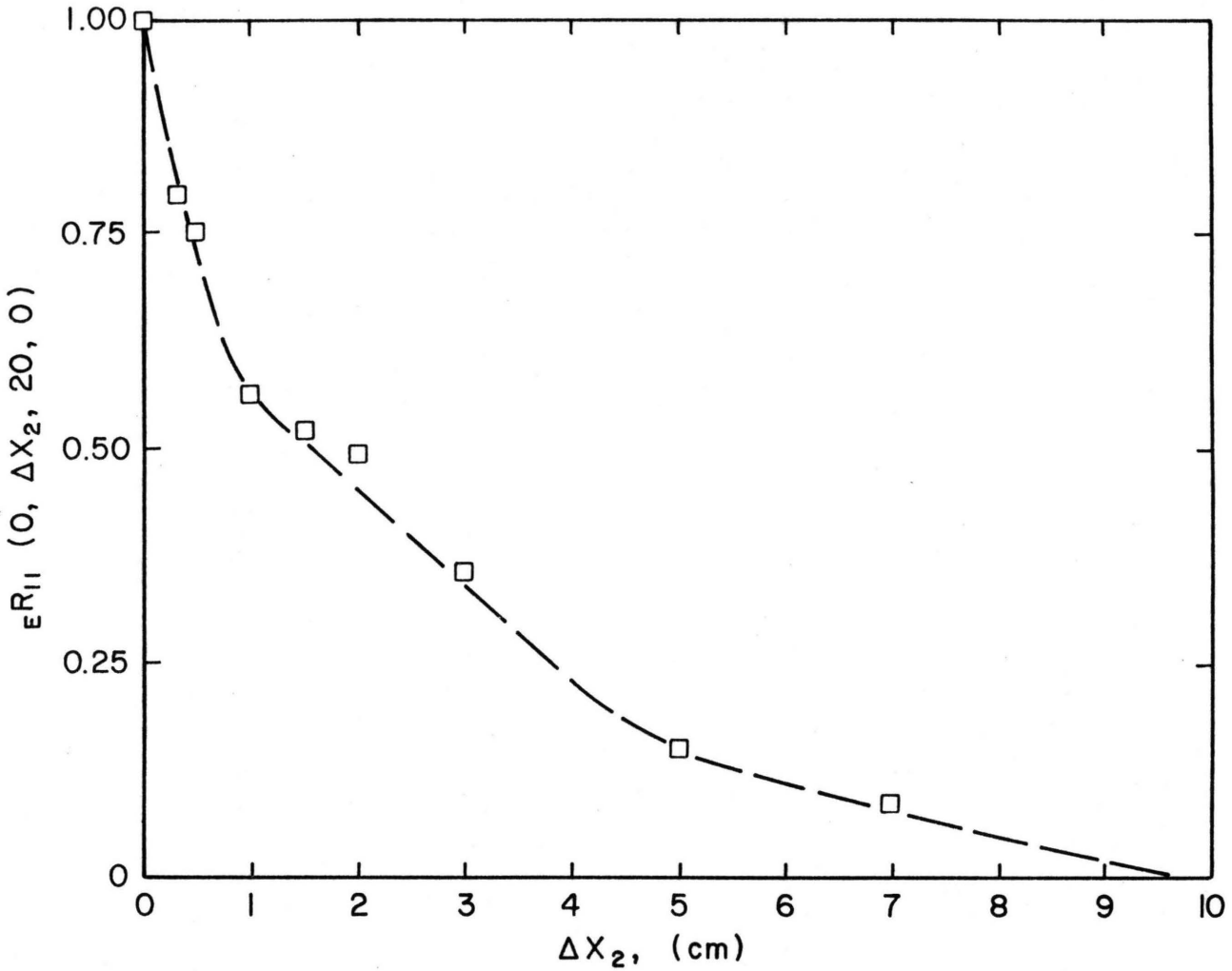

Figure 9. Transverse space correlation at 20 cm height, U_∞ = 200 cm/sec

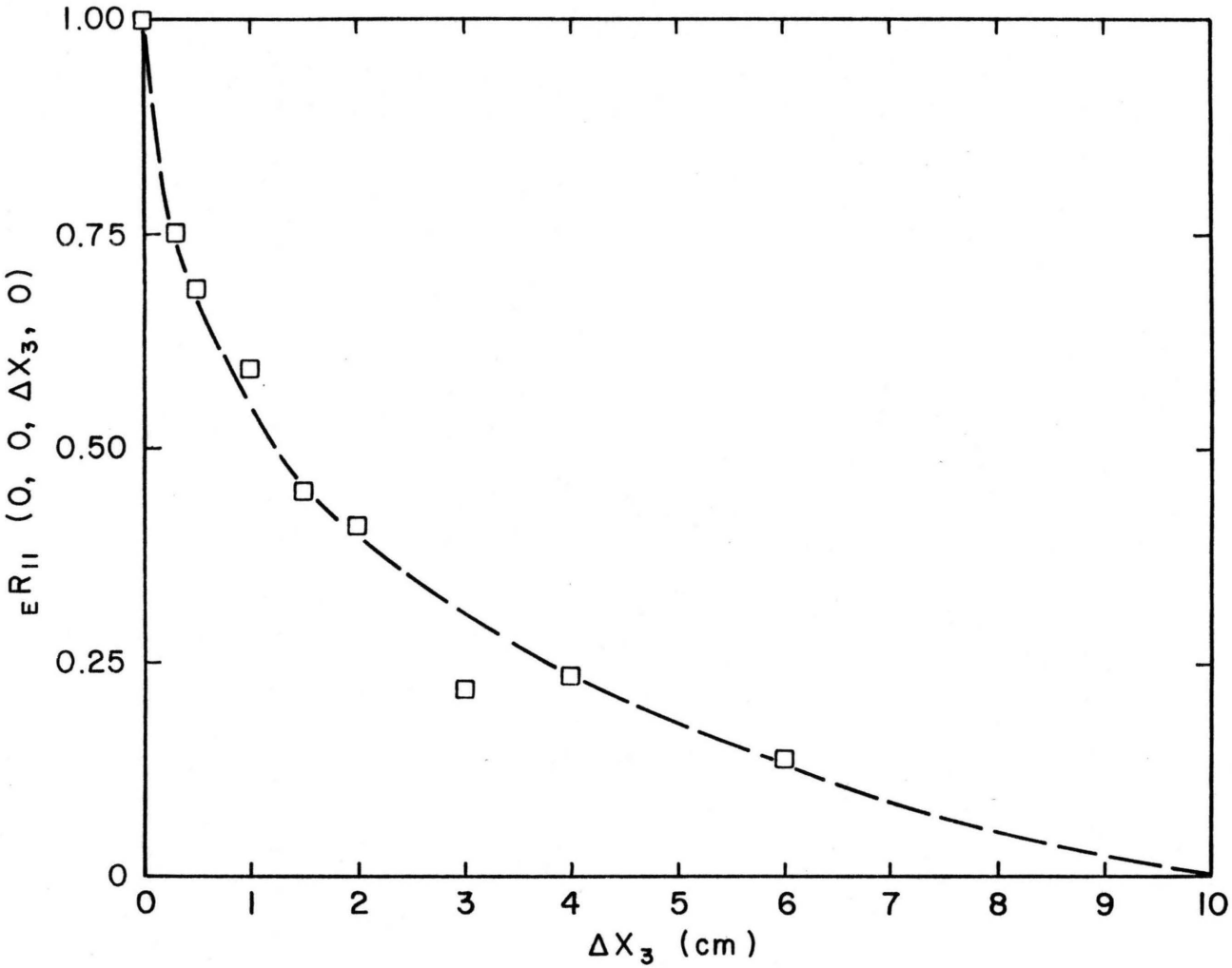

Figure 10. Vertical space correlation at 10 cm height, U_∞ = 200 cm/sec

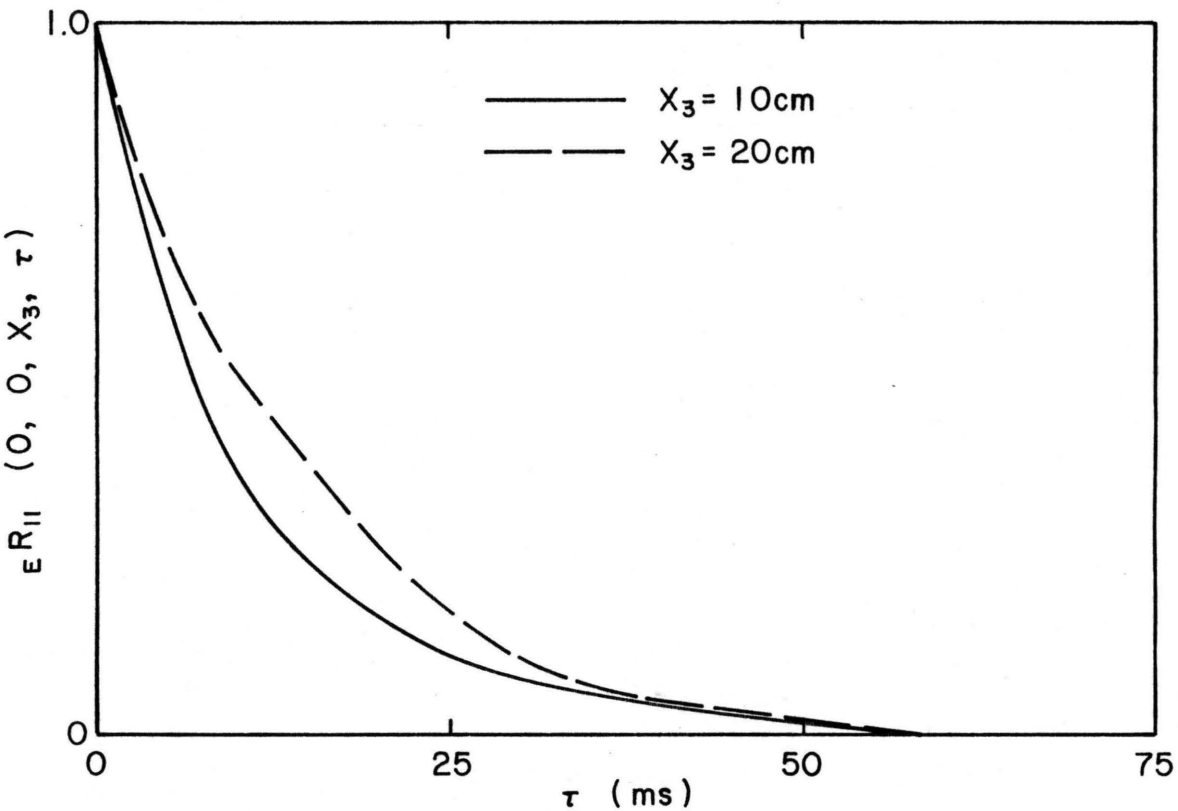

Figure 11. Longitudinal autocorrelation at 10 cm and 20 cm height

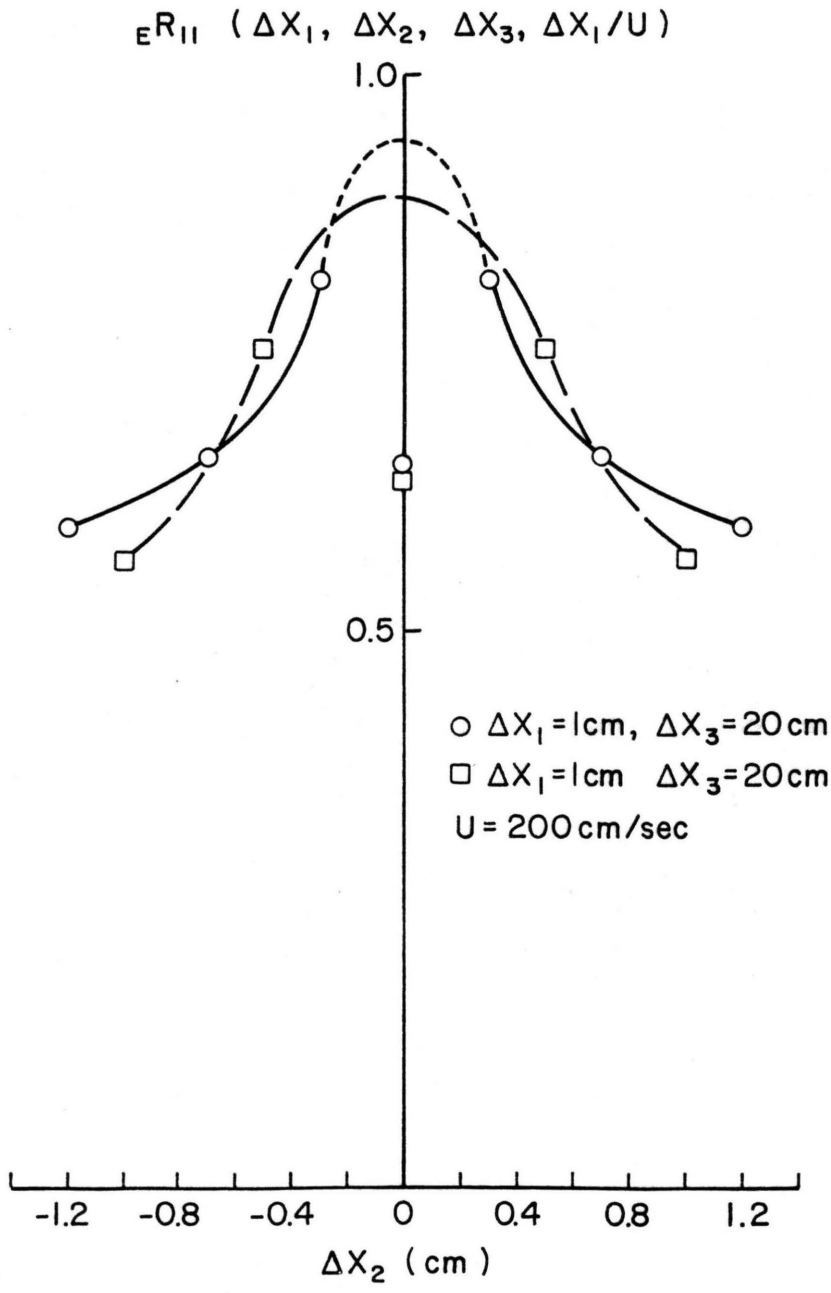

Figure 12. Longitudinal space-time correlation with transverse separations

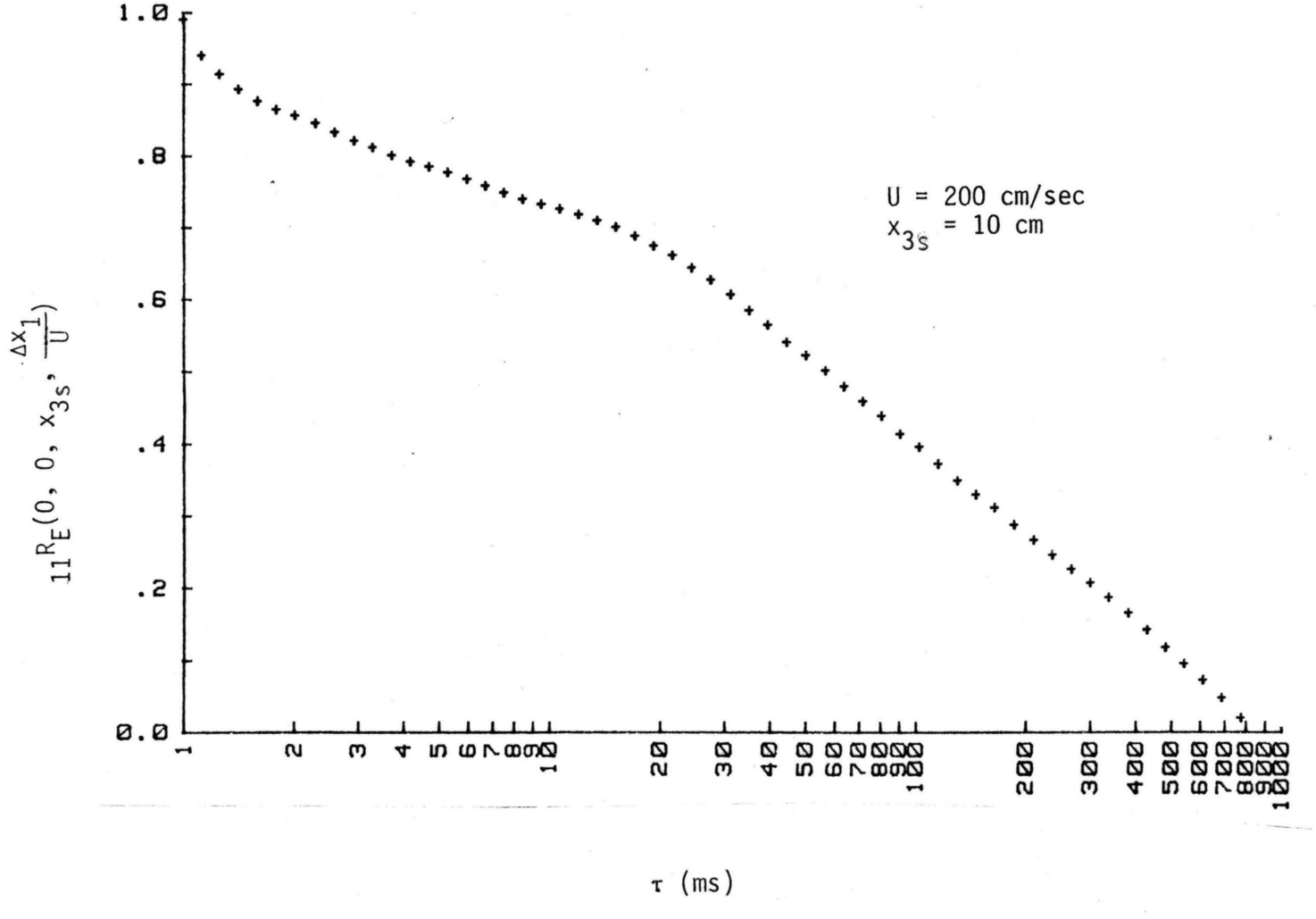

Figure 13. Longitudinal space-time correlation at 10 cm height, U_∞ = 200 cm/sec

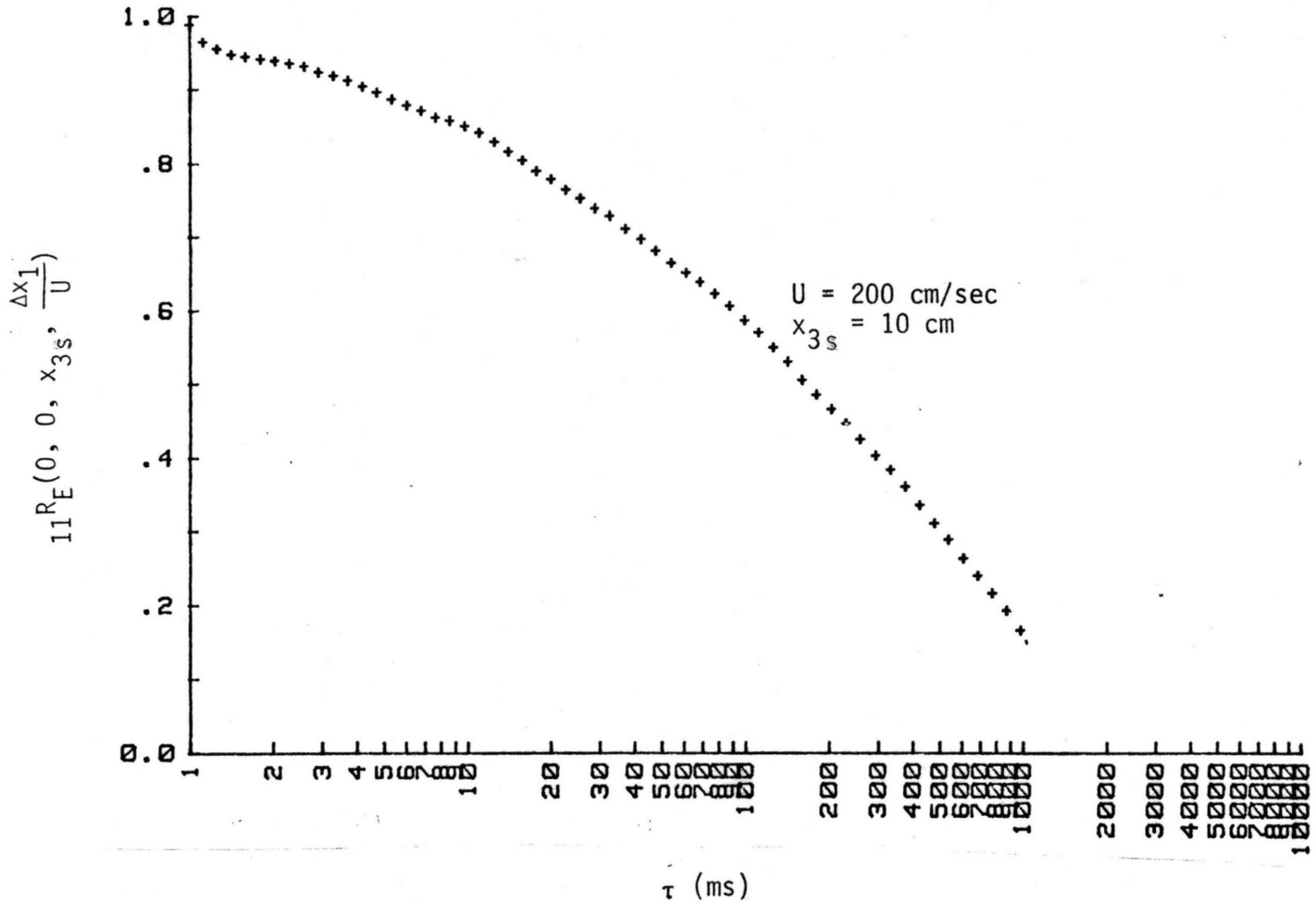

Figure 14. Longitudinal space-time correlation at 20 cm height, U_∞ = 200 cm/sec

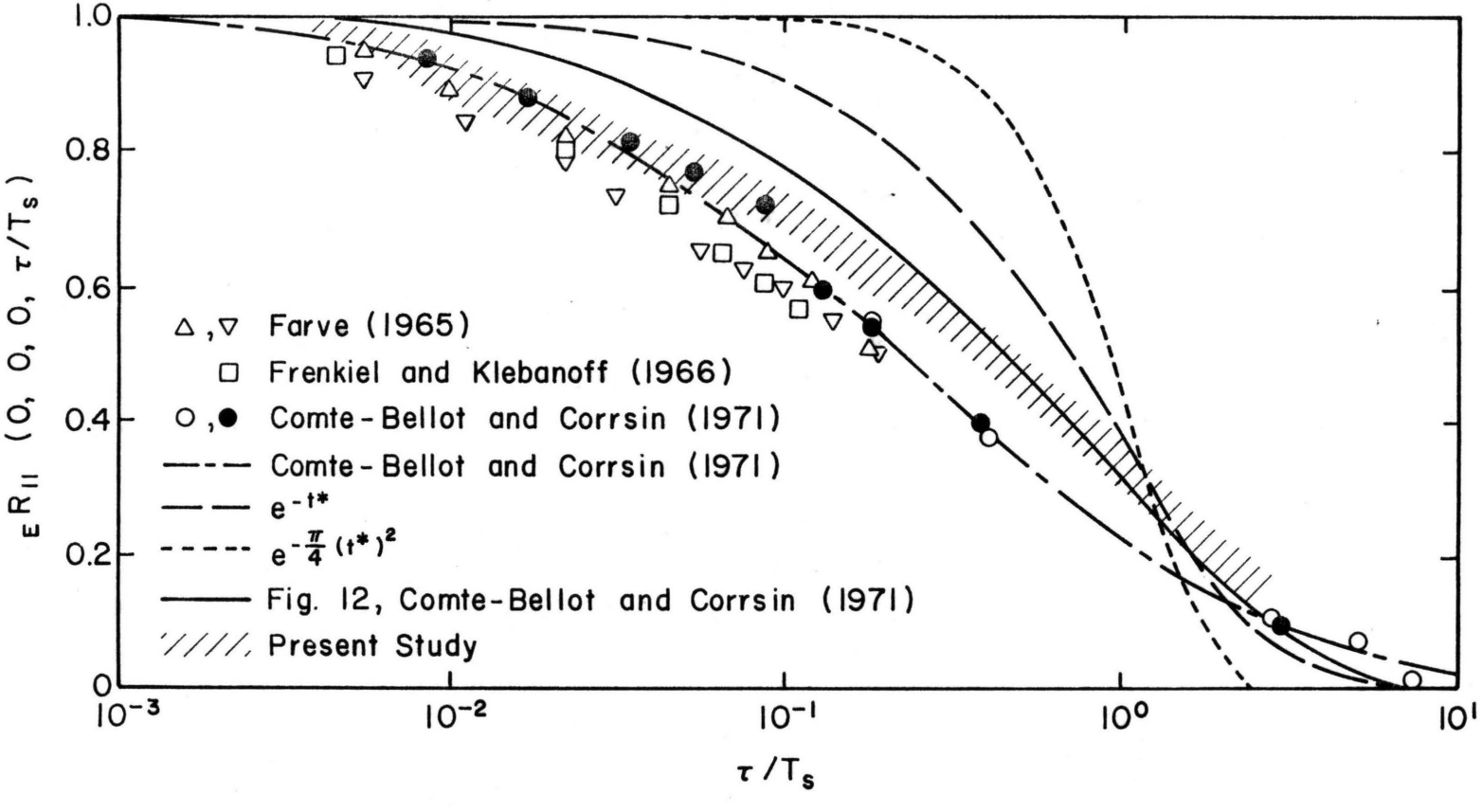

Figure 15. Normalized longitudinal space-time correlation versus τ/T_s

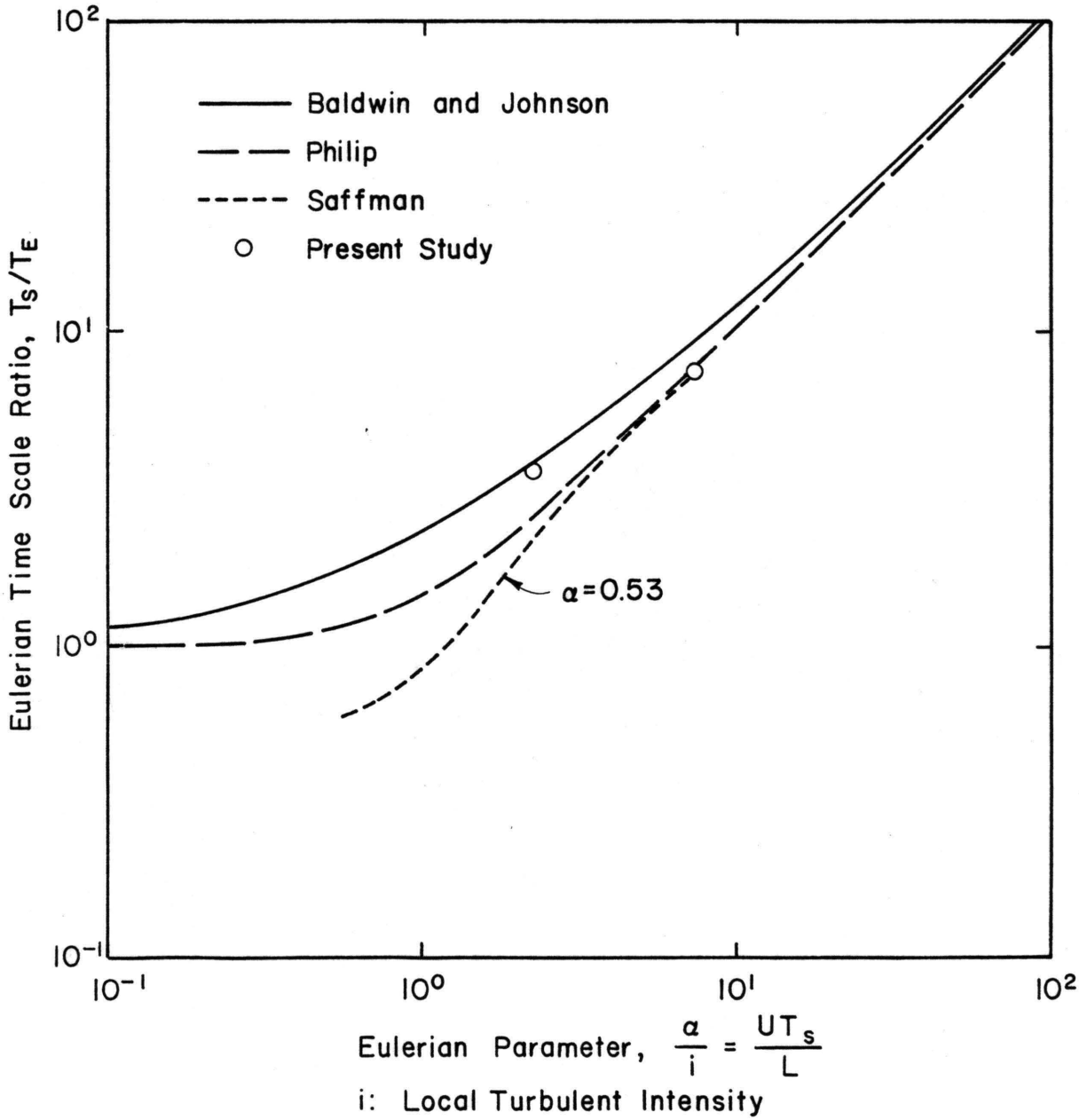

Figure 16. Properties of Eulerian models employed in the independent hypothesis analysis

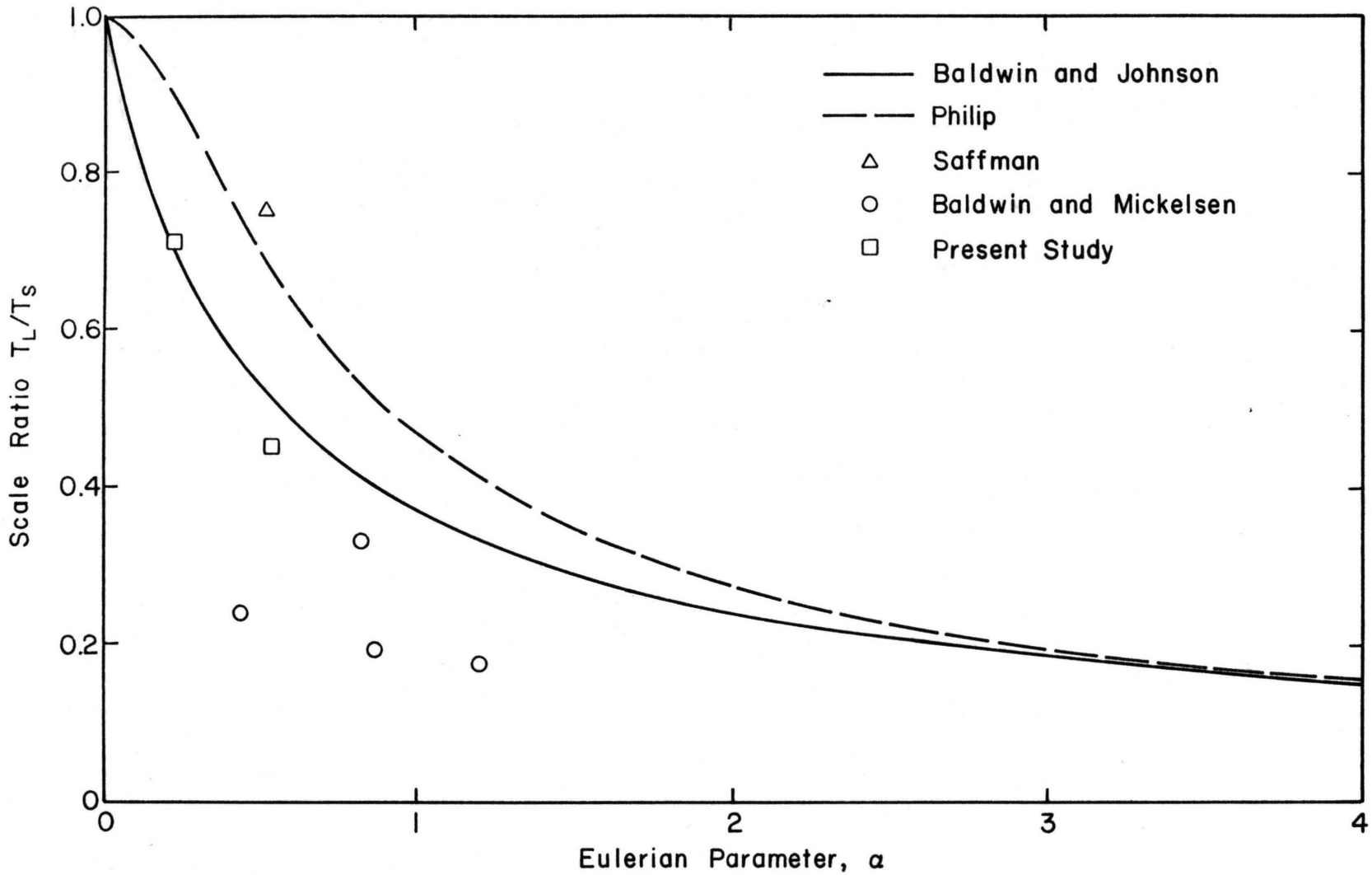

Figure 17. Lagrangian scale as a function of the Eulerian parameter